Response to Anonymous Referee #1

Dear Referee,

We thank you once more for taking the time to review our manuscript and provide valuable insights. We address reviewer comments (italic), and indicate additions or changes to the main text (blue font) as follows:

The abstract perhaps does not capture all of the important content/conclusions of the paper. It does not refer to the new methane hydrate measurement method or the new understanding of the hydrate isotopic/tracer characterization that followed from that part of the work. Can this be summarized and added? It is useful summary guidance and insight.

We have added these details, and a small elaboration of the methodology to the abstract.

P.2 line 13. The introduction summarizes the global methane debate from the point of view of sources only. The debate on sinks should perhaps be very quickly acknowledged. However, this particular line phrases a conclusion which indicates "another source than fossil fuel emissions as an explanation for recent CH4 increases". I know what the authors are trying to say here but this phrase keeps popping up in the global methane debate and it is not accurate insofar as it is self-contained, and can even be C2 ACPD Interactive comment Printer-friendly version Discussion paper very misleading to, and misused by, those with an agenda. Without fossil fuel (thermogenic) emissions in general, global methane concentrations would be declining. It is true that isotopic data etc all point to a growing proportion of biogenic emissions in the total budget recently but both source types are broadly agreed to be rising in their respective emissions - just at diverging rates (since 2006). This sentence, like so many in other papers, leads the reader to conclude that only biogenic emissions explain the recent rise - this is simply not true. All sources contribute to the rise, just in different proportions. And as I have said above, without thermogenic emissions, methane would be declining. So, this sentence is wrong, misleading and a disservice to the policy implications of the wider global methane debate. It must stop. Yes - biogenic sources are increasing, but no - they are not solely responsible for the recent rise in burden. The causes of the rise are agreed to be more convoluted than this simple conclusion suggests. Please could the authors improve the accuracy of this contextual statement in their intro?

We agree with the reviewer that some important subtleties in the possible explanations for recent trends in CH_4 need to be mentioned in our introduction, which we have modified accordingly.

We now include the following statement in the introduction (evidence from atmospheric isotopic shifts):

For example, Nisbet et al, 2016 report that the increases in CH_4 concentrations since 2005 have been accompanied by a negative shift in $\delta^{13}C$ in CH_4. Because fossil fuels have $\delta^{13}C$ in CH_4 above the atmospheric background, this negative shift implies changes in the balance of sources and sinks. I.e., even if fossil fuel emissions are partly responsible for the increases in the CH_4 atmospheric mixing ratio since 2005, their relative contribution has decreased. This suggests a role for emissions from methanogenic bacteria in wetland soils and/or ruminants, since these do have strongly negative $\delta^{13}C$ in CH_4 compared to ambient values and fossil sources, or changes in the sink strength (reaction with hydroxyl radicals, OH).

We have further modified our statement

"However, this ethane increase is weaker and less consistent than that of CH4 itself (Helmig et al., 2016), indicating another source than fossil fuel emissions as an explanation for recent CH4 increases, as well as a lack of consensus as to which sources are predominantly responsible for the increase in the CH4 mixing ratio."

To

"However, this ethane increase is weaker and less consistent than that of CH_4 itself (Helmig et al., 2016), again implicating another source than fossil fuel emissions as an explanation for most of the recent CH_4 increases, as well as a lack of consensus as to which sources are predominantly responsible for the increase in the CH_4 mixing ratio."

3/ P.10, line 18: The conclusion/statement that seafloor venting is a very small influence on climate change is a bit of an extrapolation. The calculated flux is for the seep region in the European Arctic Ocean but the conclusion made here reads as though this applies generally for the planet. Seeps in other areas may be much larger - we don't know this yet. We cannot yet say if seafloor venting globally is insignificant or not. This region's contribution may well be insignificant (over the duration of this study) but the conclusion made needs to reflect the limitation of its scope

We have modified this statement/ conclusion to better reflect the limitations of our study:

"Furthermore, only a change over time in the magnitude of a source will result in a climate forcing, suggesting only a very small influence of seafloor methane venting from this region on climate change at present."

Technical corrections: P.3 line 7: Change to "Ch4 fluxes (to atmosphere) were below..."

We have corrected this in the revised manuscript.

Please also see the uploaded 'tracked changes' document for a full overview of all changes made to our discussion paper.

Response to Anonymous Referee #2

Dear Referee,

We thank you once more for taking the time to review our manuscript and provide valuable insights. We address reviewer comments (italic), and indicate additions or changes to the main text (blue font) as follows:

However, they suggest that their estimated sea-air flux is a reasonable one for seepage sites. I disagree and rather think that it illustrates the offset between estimates derived from atmospheric data and estimates from oceanic data. The comparison with the Eastern Siberian shelf with water depth of 20-50 m water depth ignores that the proposed source region described by Geissler et al. (2016) is located in ~170 m water depth. Bubble dissolution, water column stratification, and microbial oxidation would significantly diminish methane concentration in the surface mixed layer above bubble emission sites in water depth >100 m as was shown by e.g. McGinnes et al. (2006), Mau et al. (2012), and Graves et al. (2015). The calculated high surface concentration (555 ± 297 nM) in an area of ~170 m water depth is rather unlikely. Especially, as the sea-air fluxes mentioned in the introduction (page 3, line 6-9), similar findings by Damm et al. (2007) and Mau et al. (2017), and the values mentioned in Geissler et al. (2016) indicate much lower methane concentrations and thus fluxes. Overall, there is no definite link between the atmospheric methane peak and marine seepage. The authors should mention it as it is as well as the offset in the sea-air-flux estimates.

We agree with the reviewer that it is not possible to link the observed excursion (or any other) in the atmospheric CH_4 mixing ratio to marine seepage, since, as discussed in the manuscript, there is no tracer for gas hydrates and subsea seeps. We suggest in the manuscript that this is the most consistent explanation with respect to atmospheric parameters (hereunder the FLEXPART footprint sensitivity to the area which shows that CH4 tracks remarkably well with sensitivity to the ocean area itself and the absence of other indicators of fossil fuel or wetland sources). For this reason, we have expanded upon our discussion based on four possible explanations for the offset:

Possible explanations for this offset include: 1) errors in the estimate of required dissolved CH_4 concentrations. 2) Additional (i.e. not seep related) sources of CH_4 in the water column. 3) Water conditions unique to this location and time allowing for higher dissolved CH_4 concentrations than normal in the region. 4) That the atmospheric methane is at least partly from another source.
All of the above scenarios are possible to varying degrees. The Wanninkhoff parameterisation (Eqs. 2-8) assumes emissions over a flat surface, which would be violated in the case of wind speeds at the time of the NSE of up to 7 ms^{-1}. Another source of error in the Cw estimation might be differences in wind speed over the seep site and measured at the RV Helmer Hanssen. Furthermore, while uncertainties in the required C_W are large, it should be noted that extreme values of dissolved methane (e.g. $>10^9$ nmol L^{-1}) are obtainable from Eq. 2 for a net positive flux as wind speeds (and hence gas transfer velocity) approach zero. This nonlinear effect of wind speed is also evident in Fig. S5 which shows that the dissolved CH_4 required to produce the estimated ocean-atmosphere flux increases rapidly as the wind speed drops from 7 m s^{-1} to close to 1 m s^{-1}. I.e. the offset between previously observed dissolved CH4 concentrations is small compared to what is obtainable via Eq. 2.

Other sources of marine CH_4 are also possible since the area was covered by close drift ice only one week prior to our observations, and some open drift ice was still present in the area at the time of the measurements (Fig. S6). If any CH_4 is trapped under ice during winter, it may suddenly be released when the ice melts or is blown away. For example, Kort et al. (2012) report similar ocean-atmosphere CH_4 fluxes to those in this work of up to 2 mg d^{-1} m^{-2} (23 nmol m^{-2} s^{-1}) from observations of atmospheric CH_4 at Arctic sea-ice margins and ice leads. Meanwhile, Thornton et al. (2016) estimate that relatively

high short lived CH_4 fluxes from the East Siberian Sea occur around melting ice, at 11.9 nmol m^{-2} s^{-1} (ice melt) vs 2.7 nmol m^{-2} s^{-1} (ice free).

Meanwhile, a higher dissolved CH_4 concentration than observed West of Svalbard might be due to rather low water temperatures at the North Svalbard site. We measured a water temperature of 0.7 °C for the area, vs 2-5°C for shallow waters west of Svalbard, which might result in reduced CH_4 oxidation rates by methanotrophic bacteria, generally the main factor controlling CH_4 concentrations in the water column (Graves et al., 2015). Furthermore, lateral transport of CH_4 by ocean currents is also an important factor controlling dissolved concentrations and can be expected to vary by location (Steinle et al., 2015).

Finally, we cannot rule out other sources of CH_4 to the atmosphere, since there might be responsible for the observed excursion. This might be because of error in the footprint sensitivity field and or an extremely large flux in areas of low sensitivity. In summary therefore, there is no way definitively prove, with available information that the NSE is due to ocean emissions, even if the evidence in favour is strong. Note that if there is no flux from the ocean, then the values in Table 1 can be considered as a constraint (maximum flux consistent with observations) on the CH_4 ocean atmosphere flux at this location.

We have also included references to McGinnes at al. and Mau et al. in the discussion.

I recommend including if the methane increase in the Arctic research area is higher or lower than the global increase of atmospheric methane in the abstract.

This comparison has been added to the abstract:

We show that the mean atmospheric CH_4 mixing ratio in the Arctic increased by 5.9 ± 0.38 parts per billion by volume (ppb) per year (yr^{-1}) from 2001-2017 and ~8 pbb yr^{-1} since 2008, similar to the global trend of ~7-8 ppb yr^{-1}.

Please mention that numerous papers argue against the hypothesis forwarded by Westbrook et al. (2009) that ocean warming caused the retreat of the GHSZ; one C2 of the opposing papers is the publication by Wallmann et al. (2018).

The reference to Wallmann et al. and the suggestion that the GHSZ retreat is due to isostaic shift was already included in the introduction text. However, we have slightly reworded the discussion to emphasise that there are other explanations than temperature for this GHSZ retreat:

Around Svalbard the GHSZ retreated from 360 m to 396 m over a period of around 30 years, possibly due to increasing water temperature (Westbrook et al., 2009), though numerous other sources dispute this, for example Wallmann et al., 2018 suggest that the retreating GHSZ is due to geologic rebound since the regional ice sheets melted (isostatic shift).

Consider an independent interpretation of the summer and winter atmospheric methane concentrations. What increases are higher, the summer or the winter ones? This might help to distinguish what source (anthropogenic emissions or wetlands) dominates.

We find no significant difference between the seasons concerning the trend (Fig. 1). We include this information in the revised manuscript as follows:

We find no significant difference between trends when calculated on a seasonal basis.

Exhaust emission were excluded from the on-board collected methane concentrations by removing spikes of CO2 that occur with CH4 perturbations. Do you mean increasing or decreasing CH4 concentrations?

Typically, exhaust emissions are seen to decrease CH_4 concentrations. On the other hand, this is likely to vary with engine operating conditions etc. and hence all perturbations coinciding with CO_2 spikes were removed.

Typos and figures: often CH_4 and *CO_2 are written without the numbers to be subscript*

We have now gone through all occurrences of CO_2 and CH_4 using Ctrl+F to correct this (excluding the reference section).

Please also see the uploaded 'tracked changes' document for a full overview of all changes made to our discussion paper.

instead of Hartmann et al., 2013, reference IPCC

D. L. Hartmann is the lead author of Chapter 2, the assessment report on atmospheric observations, itself part of working group one of the IPCC. I.e. we cite only Chapter 2 as instructed in the report to WG1 on pg. 159
(https://www.ipcc.ch/pdf/assessment-report/ar5/wg1/WG1AR5_Chapter02_FINAL.pdf):

This chapter should be cited as: Hartmann, D.L., A.M.G. Klein Tank, M. Rusticucci, L.V. Alexander, S. Brönnimann, Y. Charabi, F.J. Dentener, E.J. Dlugokencky, D.R. Easterling, A. Kaplan, B.J. Soden, P.W. Thorne, M. Wild and P.M. Zhai, 2013: Observations: Atmosphere and Surface. In: Climate Change 2013: The Physical Science Basis. Contribution of Working Group I to the Fifth Assessment Report of the Intergovernmental Panel on Climate Change [Stocker, T.F., D. Qin, G.-K. Plattner, M. Tignor, S.K. Allen, J. Boschung, A. Nauels, Y. Xia, V. Bex and P.M. Midgley (eds.)]. Cambridge University Press, Cambridge, United Kingdom and New York, NY, USA.

However to make it clear we a citing part of the IPCC without the reader having to look at the reference list, we will now include both references.

page 2, line 34: . . .can store large amounts of CH4 under low temperature. . ., no comma before temperature

This has been corrected in the revised manuscript

page 5, line 8: The data were collected is a harmonized way with those. . . odd sentence, correct for better readability

Here there was a typo in the manuscript. We have corrected this to

The data were collected in a harmonised way with those from the Zeppelin Observatory.

page 7, line 29: These regions are responsible for 20% of the world's natural gas and leak rates may be as high as 10%...' odd sentence

We have corrected this sentence to include the word 'production'

These regions are responsible for 20% of the world's natural gas production and leak rates may be as high as 10% (Hayhoe et al., 2002;Thompson et al., 2017).

page 10, line 6: change to: Pisso et al. (2016) describe

This has been corrected in the revised manuscript.

page 10, line 15: correct Yr-1 to yr-1

This has been corrected in the revised manuscript.

page 11, line 22: as far as I know, submitted papers are not allowed to cite

We have removed the reference to Silyakova et al. and replaced it with a reference to Graves et al. (2015) who report surface water concentrations <52 nmol L^{-1}

page 11, line 31f: reword sentence as it includes the word 'reasonable' several times

We no longer include this sentence in the revised manuscript.

page 12, line 27 and 29: change Serov et al., 2017 to Serov et al. (2017)

This has been corrected in the revised manuscript.

page 13, line 23: delete 'od' in the sentence starting with 'Using a C1/(C2+C3) ratio for

gas hydrates..'

This has been corrected in the revised manuscript.

page 15, line 25: δ missing in front of 13C-CH4

This has been corrected in the revised manuscript.

Fig. 1: smaller dots and triangles, these are as big as an island in the figure

Here we do not agree that smaller markers would be beneficial, since this would make them more difficult to see. At the same time, in the present version geographical details, i.e. the general location of the sample locations are not obscured by the markers.

Fig. 4B: 60◦N instead of 60N and rename the legend to anthropogenic, wetland, and biomass burning

We have made these changes to the figure.

Fig. 5: use same scale from 1800 to 2020 ppb CH4 for all four figures, otherwise

looking at the graphs can lead to misinterpretation

We do not agree that using the same scale would be beneficial, since the larger changes due to seasonal variation would obscure changes as a function of location, e.g. all summer measurements would appear as blue, and higher observed concentrations close to settlements on Svalbard would not be evident.

Please also see the uploaded 'tracked changes' document for a full overview of all changes made to our discussion paper.

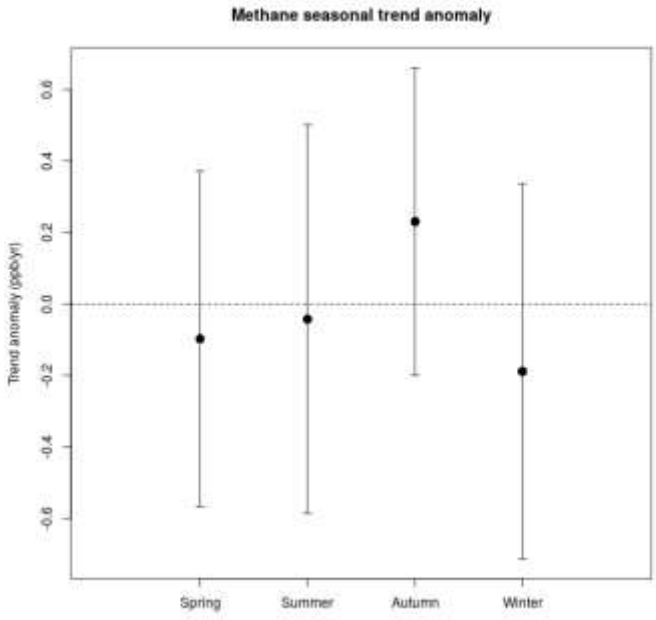

Figure 1: Seasonal trend anomalies (difference between seasonal and annual trend given by the dashed line) of methane at the Zeppelin observatory 2001-2017. Error bars represent one standard deviation.

Response to Interactive comment 'questions to be answered', Leonid Yurganov

We thank Rd. Leonid Yurganov for his insightful comments on our manuscript. We address his comments (italic), and indicate additions or changes to the main text (blue font) as follows.

Zeppelin data. Continuous precise measurements of trace gases are necessary for identification of their sources and analysis of short-term variations is important. The authors are correct considering the site itself as a really remote one and hardly affected by terrestrial sources. This is an advantage. A disadvantage is its height above sea level: 476 m. This means that a part of time it is inside Boundary Layer (BL) and a part of time it is outside it. In this concern a difference in day-by-day variability between summer and winter should be analyzed and explained: practically no variations in summer and 30-50 ppb variations in winter. There may be at least two explanations of this: a) strong emission from the sea in winter and negligible flux in summer; b) different heights of BL in summer and winter.

We consider a detailed analysis of the long-term Zeppelin dataset beyond the scope of this study, since it was used here only to provide context for our work by highlighting the regional increasing trend in CH_4 concentrations, and to expose unexplained baseline CH_4 excursions in the RV Helmer Hanssen time series. This does not preclude a future, more detailed, study on the Zeppelin methane data, which would no doubt be of great benefit to the scientific community. Furthermore, as pointed out, one of the difficulties in using Zeppelin data to investigate local emissions is of course that the station can be above the boundary layer. It is for this reason that we have primarily used RV Helmer Hanssen data in our study. Any day-to-day variations due to marine flux should be even more apparent in the RV Helmer Hanssen data. However, in the entire RV Helmer Hanssen time series we only found one short-term variation suggestive of a marine flux. We investigated it extensively (Section 3.4 in the main text). Finally, we note that baseline excursions are also higher in winter than in summer for a number of trace gases, e.g. benzene (Fig.1), such that winter variations in methane do not support the hypothesis of increased marine emissions since benzene has the same pattern but is highly unlikely to be of marine origin.

Also about Zeppelin data. The wintertime excursions surprisingly vanished in winters 2010/11 and 2011/12. No explanations have been given.

All methane data for the time series shown in Fig. 2 in the manuscript are publicly available on ebas.nilu.no. This includes data flagged as erroneous, and hence not included in the trend calculations or shown in the figure.

Another effect is overlooked: a change in methane trend around 2014, that is observed by IASI satellite instrument, as well as on the global NOAA/ESRL network (Yurganov, Leifer, Vadakkepuliyambatta, 2017).

It is true that the methane growth in the latitudinal zone north of 50°N has tended to lag the rest of the world since 2008. The reasons for this difference are a worthy target for future investigation. However, such an investigation requires an understanding of the global sources and sinks of methane (since we are interested in the comparison between the Arctic and the rest of the planet), likely necessitating extensive modelling, isotope studies etc. that we consider well beyond the scope of this study.

Sea/air flux. A very important point is relative roles of bubbles and turbulent transport in the seawater column for the total methane flux. A blocking effect of the thermocline seems to be decisive for the turbulent transfer (excluding cases of mixing by storms, that may disturb the stable surface layer). On the contrary, methane bubbles are expected to go through this barrier easily. In this case short term (on hourly basis) methane spikes must be similarly observable in summer and in winter, but longer term positive (of a few days and weeks) anomalies are expected only if the water column is well-mixed, i.e., in winter. I have not found a discussion of this in the paper.

Several studies have noted that bubbles are a poor transport mechanism for methane to the surface layer (McGinnis et al., 2006;Mau et al., 2017;Graves et al., 2015). It is likely that small bubbles released from the sea floor dissolve before reaching the surface, so these are not effective for methane transport. Large bubbles of >20 mm are likely to reach the surface intact. However, the composition of bubble released from the sea floor is not static, since gases are exchanged with the water column. Hence, a 20 mm methane bubble released at the sea floor at 100 m depth is likely to contain <1% of its original methane by the time it reaches the surface, and bubbles from even greater depths will contain a methane fraction close to that of the atmosphere (McGinnis et al., 2006). We have now included some discussion of this in section 3.4 of the revised manuscript:

However, the emissions reported for ESAS were over shallow water, and bubble dissolution, gas exchange, water column stratification, and microbial oxidation would significantly diminish CH_4 concentrations in the surface mixed layer above bubble emission sites in water depth >100 m (McGinnis et al., 2006;Mau et al., 2017;Graves et al., 2015).

Please also see the uploaded 'tracked changes' document for a full overview of all changes made to our discussion paper.

References

Graves, C. A., Steinle, L., Rehder, G., Niemann, H., Connelly, D. P., Lowry, D., Fisher, R. E., Stott, A. W., Sahling, H., and James, R. H.: Fluxes and fate of dissolved methane released at the seafloor at the landward limit of the gas hydrate stability zone offshore western Svalbard, Journal of Geophysical Research: Oceans, 120, 6185-6201, 2015.

Mau, S., Römer, M., Torres, M. E., Bussmann, I., Pape, T., Damm, E., Geprägs, P., Wintersteller, P., Hsu, C.-W., and Loher, M.: Widespread methane seepage along the continental margin off Svalbard-from Bjørnøya to Kongsfjorden, Scientific reports, 7, 42997, 2017.

McGinnis, D. F., Greinert, J., Artemov, Y., Beaubien, S., and Wüest, A.: Fate of rising methane bubbles in stratified waters: How much methane reaches the atmosphere?, Journal of Geophysical Research: Oceans, 111, 2006.

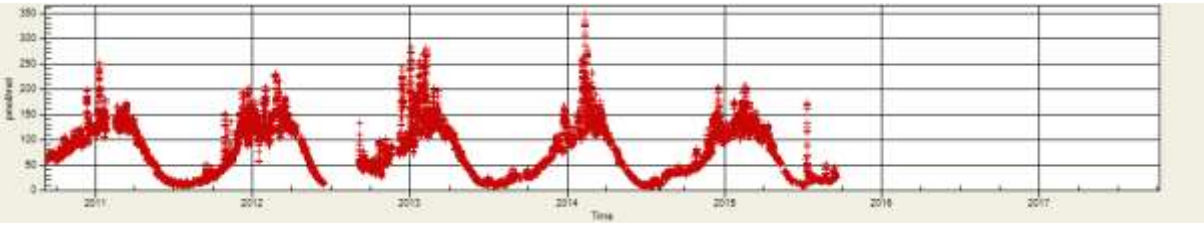

Figure 1: A screenshot of 5 years of benzene concentrations at the Zeppelin Observatory at 2h resolution. Concentrations measured using online gas chromatography. Please see ebas.nilu.no for more details.

Methane at Svalbard and over the European Arctic Ocean

Stephen M. Platt[1], Sabine Eckhardt[1], Benedicte Ferré[2], Rebecca. E. Fisher[3], Ove Hermansen[1], Pär Jansson[2], David Lowry[3], Euan G. Nisbet[3], Ignacio Pisso[1], Norbert Schmidbauer[1], Anna Silyakova[2], Andreas Stohl[1], Tove M. Svendby[1], Sunil Vadakkepuliyambatta[2], Jürgen Mienert[2], Cathrine Lund Myhre[1]

[1] NILU - Norwegian Institute for Air Research, PO Box 100, 2027 Kjeller, Norway
[2] CAGE-Centre for Arctic Gas Hydrate, Environment and Climate, Department of Geosciences, UiT The Arctic University of Norway, 9037 Tromsø, Norway
[3] Department of Earth Sciences, Royal Holloway, University of London, Egham, UK

Correspondence to: Stephen M. Platt (sp@nilu.no)

Abstract. Methane (CH_4) is a powerful greenhouse gas and atmospheric mixing ratios have been increasing since 2005. Therefore, quantification of CH_4 sources is essential for effective climate change mitigation. Here we report observations of the CH_4 mixing ratios measured at Zeppelin Observatory (Svalbard) in the Arctic and aboard the Research Vessel (RV) Helmer Hanssen over the Arctic Ocean from June 2014 to December 2016, as well as the long-term CH_4 trend measured at the Zeppelin Observatory (Svalbard) from 2001-2017. We investigated areas over the European Arctic Ocean to identify possible hot spot regions emitting CH_4 from the ocean to the atmosphere, and used state-of-the-art modelling (FLEXPART) combined with updated emissions inventories to identify CH_4 sources. Furthermore, we collected air samples in the region as well as samples of gas hydrates, obtained from the sea floor which we analysed using a new technique whereby sublimed hydrate gases are sampled directly into evacuated canisters, ~~developed as part of this work~~. Using this new methodology, we evaluated the suitability of ethane and isotopic signatures ($\delta^{13}C$ in CH_4) as tracers for ocean-to-atmosphere CH_4 emission. We found that the average methane/ light hydrocarbon (ethane and propane) ratio is an order of magnitude higher for the same sediment samples using our new methodology compared to previously reported values, 2379.95 vs 460.06, respectively. Meanwhile, w~~W~~e show that the mean atmospheric CH_4 mixing ratio in the Arctic increased by 5.9 ± 0.38 parts per billion by volume (ppb) per year (yr^{-1}) from 2001-2017 and ~8 pbb yr^{-1} since 2008, similar to the global trend of ~7-8 ppb yr^{-1}. ~~Meanwhile most~~Most large excursions from the baseline CH_4 mixing ratio over the European Arctic Ocean are due to long-range transport from land-based sources, lending confidence to the present inventories for high latitude CH_4 emissions. However, we also identify a potential hot spot region with ocean-atmosphere CH_4 flux North of Svalbard (80.4°N, 12.8°E) of up to 26 nmol m^{-2} s^{-1} from a large mixing ratio increase at the location of 30 ppb. Since this flux is highly consistent with previous constraints (both spatially and temporally), there is no evidence that the area of interest North of Svalbard is unique in the context of the wider Arctic. Rather, that the meteorology at the time of the observation was unique in the context of the measurement time series, i.e. we obtained, over the short course of the episode, measurements highly sensitive to emissions over an active seep site, without sensitivity to land based emissions.

1 Introduction

The atmospheric mixing ratio of methane (CH_4), a powerful greenhouse gas with global warming potential ~32 times higher than carbon dioxide (CO_2) (Etminan et al., 2016), has increased by over 150% since pre-industrial times (Hartmann et al., 2013;)(IPCC, 2013). The CH_4 mixing ratio increased significantly during the 20th century, and then stabilised from 1998-2005. This brief hiatus ended in 2005 and the mixing ratio has been increasing rapidly ever since (Hartmann et al., 2013;)(IPCC, 2013). For example, the global mean CH_4 mixing ratio was 1953 ppb in 2016, an increase of 9.0 ppb compared to the previous year (WMO 2017). An ~8-9 ppb increase per year in atmospheric CH_4 is equivalent to net emissions increase of ~25 Tg CH_4 per year (Worden et al., 2017).

The reasons for the observed increases in atmospheric CH_4 are~~is~~ unclear. A probable explanation, identified via shifts in the atmospheric $\delta^{13}C$ in CH_4 isotopic ratio compared to the Vienna Pee Dee Belemnite standard ($\delta^{13}C$ in CH_4 vs V-PDB) is increased CH_4 emissions from wetlands, both in the tropics (Nisbet et al., 2016) as well as in the Arctic (Fisher et al., 2011). For example, Nisbet et al, 2016 report that the increases in CH_4 concentrations since 2005 have been accompanied by a negative shift in $\delta^{13}C$ in CH_4. Because fossil fuels have $\delta^{13}C$ in CH_4 above the atmospheric background, this negative shift implies changes in the balance of sources and sinks. I.e., even if fossil fuel emissions are partly responsible for the increases in the CH_4 atmospheric mixing ratio since 2005, their relative contribution has decreased. This suggests a role for emissions from methanogenic bacteria in wetland soils and/or ruminants, since these do have strongly negative $\delta^{13}C$ in CH_4 compared to ambient values and fossil sources, or changes in the sink strength (reaction with hydroxyl radicals, OH).

There is also evidence that the fraction of CH_4 emitted by fossil fuels is higher than previously thought, based on mixing ratios of co-emitted ethane (Worden et al., 2017;Dalsøren et al., 2018), suggesting that current emission inventories need revaluating. As well as increases in the average global CH_4 mixing ratio, ethane, often co-emitted with anthropogenic CH_4 has also increased. However, this ethane increase is weaker and less consistent than that of CH_4 itself (Helmig et al., 2016), indicating another source than fossil fuel emissions as an explanation for recent CH_4 increases, as well as a lack of consensus as to which sources are predominantly responsible for the increase in the CH_4 mixing ratio. Accordingly, it is clear that although a total net CH_4 flux to the atmosphere of ~550 Tg CH_4 yr^{-1} is well constrained via observations (Kirschke et al., 2013), the relative contribution of the individual sources and sinks responsible for the rapid increases since 2005 is uncertain (Dalsøren et al., 2016;Saunois et al., 2016;Nisbet et al., 2016), making future warming due to CH_4 emissions difficult to predict. Therefore, the recent observed increase in the atmospheric CH_4 mixing ratio has led to enhanced focus and intensified research to improve the understanding of CH_4 sources and changes particularly in response to global and regional climate change.

In this study, we focus on the Arctic, and investigate the impact of oceanic CH_4 sources on atmospheric CH_4. The Arctic region is of great importance since surface temperatures are rising at around 0.4°C per decade, twice as fast as the global average warming rate (Chylek et al., 2009;Cohen et al., 2014), and it contains a number of CH_4 sources sensitive to temperature changes. For example, high latitude (>50°N) wetlands are a significant source of Arctic CH_4, contributing as much as 15% to the global CH_4 budget (Thompson et al., 2017). Furthermore, Dlugokencky et al. (2009), ;Bousquet et al. (2011), and;Rigby

Formatted: Subscript

Formatted: English (United Kingdom)

et al. (2008) link anomalous Arctic temperatures in 2007 with elevated global CH_4 mixing ratios in the same year due to increased high latitude wetland emissions. Other Arctic CH_4 sources sensitive to temperature include forest and tundra wildfires, likely to increase in frequency and intensity with warmer temperatures and more frequent droughts (Hu et al., 2015), and thawing permafrost and tundra (Saunois et al., 2016).

Oceanic CH_4 sources, are small globally (2-40 Tg yr^{-1}) compared to terrestrial sources such as wetlands (153–227 Tg yr^{-1}) and agriculture (178–206 Tg yr^{-1}) (Saunois et al., 2016;Kirschke et al., 2013). However, oceanic CH_4 fluxes are highly uncertain and may be particularly important in the Arctic due to the extremely large reservoirs of CH_4 under the seabed, and the potential for climate feedbacks. For ~~example~~example~~, methane in~~ gas hydrates (GHs), an ice-like substance formed in marine sediments, can store large amounts of CH_4 under low~~,~~ temperature and high pressure conditions within the gas hydrate stability zone (GHSZ) (Kvenvolden, 1988). Around Svalbard the GHSZ retreated from 360 m to 396 m over a period of around 30 years, ~~either~~ possibly due to increasing water temperature (Westbrook et al., 2009), though numerous other sources dispute this, for example Wallmann et al., 2018 suggest that the retreating GHSZ is due to geologic rebound since the regional ice sheets melted (isostatic shift). ~~and/or decreasing sea levels following geologic rebound as the regional ice sheets melt (isostatic shift) (Wallmann et al., 2018).~~ The climate impact of decomposing GHs is poorly constrained, in part due to large uncertainties in their extent (Marín-Moreno et al., 2016). Though Kretschmer et al. (2015) give a recent estimate of 116 Gt carbon stored in hydrates under the Arctic Ocean, other estimates vary widely, from 0.28 to 512 Gt carbon (Marín-Moreno et al., 2016, and refs therein).

Presently, little of the CH_4 entering the water column over active geologic seep sites and at the edge of the GHSZ around Svalbard reaches the atmosphere. CH_4 fluxes to the atmosphere were below 2.4 ± 1.4 nmol m^{-2} s^{-1} in summer 2014 at a shallow seep site (50-120m depth) off Prins Karls Forland (Myhre et al., 2016) and below 0.54 nmol m^{-2} s^{-1} for all waters less than 400 m deep around Svalbard in 2014-2016 (Pisso et al., 2016). Such low ocean-atmosphere CH_4 fluxes, even over strong sub-sea sources, may be due to the efficient consumption of CH_4 by methanotrophic bacteria (Reeburgh, 2007). However, the extent to which microbiology or any other factor mitigates the climate impact of sub-sea seep sites across the wider Arctic region, and whether it will continue to do so, is uncertain. Furthermore, previous studies do not report observed fluxes since ocean-atmosphere emissions were too low to produce observable changes in atmospheric CH_4 mixing ratios. Either, flux constraints were estimated by determining the maximum flux possible which would not exceed observed variations in the measured atmospheric CH_4 mixing ratio (Myhre et al., 2016;Pisso et al., 2016), or fluxes were inferred based on dissolved CH_4 concentrations at the ocean surface (Myhre et al., 2016;Pohlman et al., 2017). Therefore, while this suggests ocean-atmosphere fluxes are very low around Svalbard, at least for the periods so far studied, the true size of the CH_4 flux from subsea seeps and gas hydrates remains unknown.

Finally, while not sensitive to temperature changes, anthropogenic emissions are a significant source of high latitude CH_4 emissions. For example, a significant fraction of the world's oil and gas is extracted in Russia, for which Hayhoe et al. (2002) estimate CH_4 leakage rates as high as 10%. This leak rate is likely to have declined substantially in recent years to around 2.4 % or 27.7 Mt in 2015 (UNFCC, 2018), likely due to increased recovery of associated gas (CH_4 rich gas produced during the

Formatted: Font: 10 pt

fossil fuel extraction process) and hence less flaring in the region (Höglund-Isaksson, 2017). The Norwegian coastal shelf also has a large number of facilities related to oil and gas extraction, though fugitive emissions are much lower than for Russia at only 0.04 Mt (UNFCC, 2018).

Here we report observations of CH_4 at Zeppelin Observatory from 2001-2017, and over the European Arctic Ocean from 2014-2016 measured on board the research vessel (RV) Helmer Hanssen. To identify and quantify potential oceanic CH_4 sources under present climate conditions we scanned relevant areas of the Arctic Ocean to identify hot spot regions. In this time period the RV Helmer Hanssen passed in close proximity to known sub-sea CH_4 seeps, the edge of the GHSZ at several locations, Arctic settlements such as Longyearbyen (Svalbard), the Norwegian and Greenland coasts, and oil and gas facilities in the Norwegian Sea. Using these data combined with other available information, i.e. carbon dioxide (CO_2), FLEXPART modelled source contributions, data from the Zeppelin Observatory, we observe and explain episodes of increased CH4 over the Arctic Ocean, thereby evaluating the emission inventories and investigating whether seeps or decomposing hydrates influence atmospheric CH_4 mixing ratios. We also utilise the $\delta^{13}C$ in CH_4 vs V-PDB and atmospheric mixing ratios of light hydrocarbons (LHC, i.e. ethane, propane) in the atmosphere above and around known subsea seep sites and compare this to the composition of GHs from sediment core samples. For this comparison, we developed a new methodology to obtain GH samples for laboratory analysis.

Formatted: Subscript

Formatted: Subscript

2 Methodology

2.1 Methane measurements at the Zeppelin Observatory

The Zeppelin observatory (78.91°540 N, 11.89° E) is located at the Zeppelin Mountain (476 m above sea level, asl) on the island of Spitsbergen (the largest island of the Svalbard archipelago, Fig. 1) and has an atmospheric CH_4 mixing ratio record dating from 2001. The observatory is a regional background site, far from local and regional sources (Yttri et al., 2014). Data from Zeppelin contribute to global, regional and national monitoring networks, including the European Evaluation and Monitoring Programme (EMEP), the Global Atmospheric Watch (GAW), the Arctic Monitoring and Assessment Programme (AMAP), and Advanced Global Atmospheric Gases Experiment (AGAGE). The site is also included in the EU infrastructure project ACTRIS (Aerosols, Clouds and Trace gases Research InfraStructure). In May 2018, Zeppelin was classified as ICOS (Integrated Carbon Observation System) class 1 site for CO_2, CH_4 and CO measurements.

For 2001-2012 we obtained CH_4 measurements with a gas chromatography flame ionisation detector (GC-FID) system with an inlet 2 m above the observatory roof (i.e. 478 m asl). Sample precision for this system was ±3 ppb at hourly resolution as determined from repeat calibrations against Advanced Global Atmospheric Gases Experiment (AGAGE) reference standards (Prinn et al., 2008). Since April 2012 we have measured CH_4 at Zeppelin using a cavity ring-down spectroscope (CRDS, Picarro G2401) at 1 minute resolution with a sample inlet 15 m above the observatory roof (491 m asl). We calibrate the CRDS every 3 days against working standards, which we calibrate to National Oceanic and Atmospheric Administration (NOAA) reference standards. For both of these sampling regimes, we sampled the air via a heated inlet with excess airflow (residence

time ~10 s) and through a Nafion drier to minimise any water correction error in the instruments. The full time series from August 2001-2013 was re-processed as a part of the harmonisation of historic concentration measurements within the European Commission project, InGOS, archived and documented in the ICOS Carbon portal (ICOS, 2018).

2.2 Trend Calculations for methane at the Zeppelin Observatory

We calculated the annual trend in atmospheric CH_4 mixing ratio according to Simmonds et al. (2006), whereby the change in atmospheric mixing ratio of a species as a function of time *f(t)* is fit to an empirical equation combining Legendre polynomials and harmonic functions with linear, quadratic, and annual and semi-annual harmonic terms for 2N months of data:

$$f(t) = a + b \cdot N \cdot P_1\left(\frac{t}{N} - 1\right) + \frac{1}{3} \cdot d \cdot N^2 \cdot P_2\left(\frac{t}{N} - 1\right) + \frac{1}{3} \cdot e \cdot N^3 \cdot P_3\left(\frac{t}{N} - 1\right) + c_1 \cdot cos(2\pi t) + s_1 \cdot sin(2\pi t). \quad (1)$$

An advantage of this methodology is that seasonal variation is accounted for, while fitting parameters *a-e* yield useful information. For example, *a* defines the average mole fraction, *b* defines the trend in the mole fraction and *d* defines the acceleration in the trend. Coefficients *c1* and *s1* define the annual cycles in the mole fraction and P_i are the Legendre polynomials of order *i*.

2.3 Atmospheric trace gas measurements at RV Helmer Hanssen

We obtained near continuous online CH_4 and CO_2 time series on board the RV Helmer Hanssen using a CRDS (Picarro G2401) from June 2014 to December 2016 (see Fig. 1 for route). The data were collected ~~is~~ in a harmonised way with those from the Zeppelin Observatory. The CRDS connects to a heated main sample inlet line with excess airflow and air is sampled through a drier. A multiport valve on the instrument inlets enables switching between sampled air and control samples/working standards. As at the Zeppelin Observatory, we calibrate the CRDS instrument every 3 days with working standards calibrated to National Oceanic and Atmospheric Administration (NOAA) reference standards. The central inlet line on the RV Helmer Hanssen is connected to the top of the mast (22.4 m asl) located to the fore of the ship exhaust (Fig. 2). Sample residence time is about 10 seconds. We manually exclude measurements affected by exhaust emissions by excluding data where spikes in the CO_2 mixing ratio of 100 ppm above background or higher coincided with perturbations in the CH_4 mixing ratio. We ~~also~~ observed no correlation between apparent wind direction relative to the bow (i.e. wind experienced by an observer on board~~, and not accounting for the ship's motion~~) ~~vs heading~~, and CH_4 mixing ratios after filtering the data in this way (Fig. S1, Supplementary Information, SI).

We also collected air samples for offline analysis on board the RV Helmer Hanssen into evacuated stainless steel canisters (see Fig. 1 for sampling locations), using the same sample line as the CRDS system (Fig. 2). We sent the canisters for analysis at the laboratory at NILU where we analysed them with a gas chromatography mass spectrometer (GC-MS) system (Medusa, Miller et al., 2008). This instrument detects trace gases including a range of hydrocarbons (e.g. ethane and propane) at the ppt

Formatted: Subscript

Formatted: Font: Italic

Formatted: Font: Italic

Formatted: Subscript

Formatted: Subscript

level and is calibrated AGAGE reference standards (Prinn et al., 2008). We separated a fraction of each of the air samples collected in 2014 at the RV Helmer Hanssen into new stainless steel flasks, which we then slightly over-pressurised with clean air and submitted for isotopic analysis ($\delta^{13}C$ in CH_4 vs V-PDB) at Royal Holloway, University of London (RHUL). CH_4 and CO_2 were first quantified using a CRDS (Picarro G1301) for quality control. Each sample was then analysed, at least in triplicate, using a Trace Gas-IsoPrime CF-GC-IRMS system (Fisher et al., 2011, and references therein), giving an average precision of 0.04 ‰. Finally, in addition to the aforementioned atmospheric parameters, we also collected meteorological and nautical data e.g. wind speed and wind direction, water temperature, ice cover, sea state etc. at the RV Helmer Hanssen.

2.4 Collection of gas hydrate samples

We obtained two sediment cores containing GHs from the sea-floor south of Svalbard on 23.05.2015, CAGE 15-2 HH 911 GC and CAGE 15-2 HH 914 GC, at 76.11°N, 15.97°E and 76.11°N, 16.03°E, respectively (Fig. 1). We immediately transferred small GH pieces (~1 cm^3) to an airtight container connected to an evacuated stainless steel flask via stainless steel tubing and a two-way valve. Once the airtight container with the GH sample was sealed, we opened the two-way valve to allow sublimated gas from the sample into the evacuated flask. This sample was then stored for subsequent analysis of light hydrocarbons (LHCs) and CH_4 at NILU, using GC-FID and a Picarro CRDS, respectively, as well as $\delta^{13}C$ at RHUL.

In a widely used GH sampling technique, small hydrate pieces are transferred into glass vials containing an aqueous sodium hydroxide (NaOH) solution and sealed with a rubber stopper (e.g. Smith et al., 2014;Serov et al., 2017). Overpressure due to gases released from the sediments is reduced by exposing the sample to the atmosphere. Our technique, developed as part of this study, offers several advantages over this methodology. Firstly, we avoid artefacts likely to occur using the headspace technique due to repeated exposure to the atmosphere and contamination from the gases initially present in the headspace. Secondly, we do not dissolve the gas samples in solution, which might otherwise change the relative concentrations of the gases since they will have different solubilities in $NaOH_{(aq)}$. Thirdly, the stainless steel connections in our GH sampling system are certified for pressures up to 120 Bar (while the flask itself has a tolerance of 150 bar), allowing for collection of a larger gas volume. Finally, the sample can be stored indefinitely and transported without gas exchange between the sample and the atmosphere since the closed valve of a stainless steel flask is relatively more secure than a rubber stopper.

2.5 Atmospheric transport modelling

We modelled atmospheric transport using a Lagrangian particle dispersion model, FLEXPART v9.2 (Stohl et al., 2005), to produce gridded (0.1×0.1 degree) sensitivity fields for surface (so called 'footprint sensitivity') CH_4 emissions 20 days backwards in time for both the RV Helmer Hanssen and Zeppelin Observatory for the Northern Hemisphere. Since the RV Helmer Hanssen is a moving platform, we generated receptor boxes at hourly time resolution, or, the time taken to move by 0.5 degrees latitude or longitude, if this was less than 1 hour, along the ship track. Thus, the minimum time resolution was 1 hour, increasing to higher time resolution when the ship was moving at relatively high speeds.

FLEXPART footprint sensitivities provide both qualitative and quantitative information. For example, inspection of the footprint provides information about which areas have more influence on measured mixing ratios, even in the absence of numerical emission data. Furthermore, the units of the FLEXPART output are such that the product of sensitivity and flux density yields the mixing ratio change at the receptor (e.g. for sensitivity in units of $kg^{-1}m^2s$ and emission flux densities in kg $m^{-2}s^{-1}$). In this study, we use footprint sensitivities to simulate the influence of terrestrial sources during the 20 days prior to sampling on CH_4 mixing ratios, as the product of footprint sensitivity and monthly gridded emission fields.

2.6 Use of emission inventories

Bottom-up estimates of anthropogenic CH_4 emissions from the main sources are taken from emission inventories, which provide estimations based on national and international activity data, sector-by-sector emission factors, and gridded proxy information for activity distribution. In this work, we used for anthropogenic emissions GAINS-ECLIPSE version 5a (Stohl et al., 2015, http://www.iiasa.ac.at/web/home/research/researchPrograms/air/ECLIPSEv5a.html) for the latest available year, 2010. For biomass burning emissions, we used data from the Global Fire Emissions Database, GFEDv4, (Randerson et al., 2017) for the year 2014. For wetland emissions we used estimates from the global vegetation and land surface process model LPX-Bern (Spahni et al., 2011;Stocker et al., 2014;www.climate.unibe.ch), also for 2014.

3 Results and discussion

3.1 Long term methane trends at Zeppelin Observatory

As discussed in Sect. 2.1 the location of the Zeppelin Observatory on an Arctic mountain is ideal for studying long-term hemispheric changes since the site is far from local and regional CH_4 sources and pollution. Nevertheless, there are episodes with long-range transport of pollution from lower latitudes from Russia, Europe and the US (Stohl et al., 2007;Stohl et al., 2013;Yttri et al., 2014). The daily mean observations of CH_4 at Zeppelin since the start in 2001 together with empirical (Eq. 1) depict a strong increase from late 2005, with a trend of 5.9 ± 0.3 ppb yr^{-1} over the period 2001-2017 (Fig. 3). There was a new record level of 1938.9 ppb in CH_4 annual mean in 2017, an increase of 6.8 ppb since 2016, and as much as 86.4 ppb increase since 2005. The global mean for 2016 was 1853 ppb (WMO, 2017) while the level at Zeppelin was 1932.1 ppb, reflecting large-scale latitudinal gradients with highest concentrations in the Arctic. Since 2010, the average yearly increase is 8 ppb at Zeppelin. We find no significant difference between trends when calculated on a seasonal basis.

Dalsøren et al. (2016) addressed the atmospheric CH_4 evolution over the last 40 years using the OsloCTM3 model, and found that for Zeppelin, wetland emissions and fossil gas emissions are the main contributors in summer and winter, respectively. The highest ambient CH_4 mixing ratio measured at Zeppelin (Fig. 3) was on the 5th December 2017, of 2016.3 ppb. The transport pattern for that day shows a strong influence from Russian industrial pollution from North-Western Siberia (NILU, 2018). Fugitive emissions from Russian gas installations are a possible source of this CH_4. However, on this particular day, both carbon monoxide (CO) and CO_2 levels were also very high, possibly implicating industrial pollution.

There is most likely a combination of reasons for the recent strong increases in CH_4 and the dominating reason is not clear. A probable explanation is increased CH_4 emissions from wetlands, both in the tropics as well as in the Arctic region, in addition to increases in emission from the fossil fuel industry. Ethane and CH_4 are emitted together from fossil oil and gas sources, and a slight decrease or stable level in ethane at Zeppelin (Dalsøren et al., 2018) supports the hypothesis that wetland emission changes are a large contributor to increasing CH_4 mixing ratios. Emissions from the ocean could also be an important factor, which we investigate in depth in this study (Sects. 3.3-3.4).

3.2 Emissions

The main high latitude source regions for anthropogenic CH_4 emission are the oil and gas fields in Arctic North West Russia and Western Siberia, particularly in the Pechora and Ob River regions (Fig. 4A). These regions are responsible for 20% of the world's natural gas production and leak rates may be as high as 10% (Hayhoe et al., 2002;Thompson et al., 2017). Furthermore, according to the GAINS-ECLIPSE model, fuel production and distribution represented the largest fraction, ~87%, of CH_4 emissions from Asian Russia. These emissions are expected to steadily increase from an estimated 12900-14400 kt CH_4 yr^{-1} between 2010 and 2030, still markedly down from an estimated 19600 kt CH_4 yr^{-1} in 1990. Some areas of Western Europe, e.g. the UK and the Netherlands are also expected to influence high latitude CH_4 mixing ratios. Western European CH_4 emissions are from waste treatment and agriculture and are expected to steadily decrease. Meanwhile, for wetland emissions, the source regions are much more widely distributed covering in particular large areas of Siberia, North West Russia, Fennoscandia, Western Europe and North America. Finally, biomass burning events tend to occur in heavily forested regions of Eastern Siberia and Canada (Fig. 4A). Wetland emissions are expected to dominate from June to September above 60°N, with anthropogenic emissions dominant for the rest of the year (Fig. 4B).

3.3 Methane at the RV Helmer Hanssen

Methane mixing ratios measured at the RV Helmer Hanssen tended to be elevated close to the Norwegian coast and around Kongsfjorden (78.75°N, 16°E, Svalbard, Fig. 5), explained by higher sensitivity to terrestrial emissions, since there are numerous settlements and fossil fuel industry installations along the Norwegian coast and in the Kongsfjorden area. Repeated instances of high CH_4 in the Barents Sea also apparent in Fig. 5 coincide with increased sensitivity to emissions from land-based sources according to FLEXPART, likely because this area is relatively close to major emissions sources.

We observed a clear link between CO_2 mixing ratios and CH_4 (Fig. 6, Fig. S2). In winter, CH_4 tends to increase together with CO_2, indicative of CH_4 produced via combustion processes, i.e. mainly from anthropogenic sources (Fig. S2). In summer, many observed CH_4 excursions coincide with decreased CO_2, typical for CH_4 from biologically active regions where photosynthesis depletes CO_2. These observations thus validate the predictions of the model and emission inventories whereby we expect anthropogenic emissions to be the largest contributor to winter variability in CH_4 mixing ratios and wetlands the largest contributor in summer (Fig. S2). We observe only one occurrence of a large CH_4 excursion (>10 ppb) throughout the

entire measurement series on 25.08.2014 without a corresponding perturbation of the Zeppelin Observatory CH_4, RV Helmer Hanssen CO_2, or FLEXPART emissions time series (Fig. 6, Fig. S2).

We assess the agreement between the Zeppelin Observatory and modelled emissions and the RV Helmer Hanssen CH_4 time series on a monthly basis in the Taylor diagrams (Taylor, 2001) in Fig. 7, which shows the R^2 correlation on the angular axis and the ratio of standard deviations (Zeppelin to RV Helmer Hanssen) on the radial axis. Monthly correlations range from 0.1 to 0.8 for both the modelled emissions and the Zeppelin Observatory, while for most months standard deviation of the Zeppelin CH_4 is below that of the RV Helmer Hanssen, likely reflecting the fact that the latter is exposed to more variable sources as a moving platform at sea level. The agreement between the model and observations is mostly above R^2=0.3, as Thompson et al. (2017) also report for a number of high latitude measurement stations. For some months, the correlation between the model and observations is strikingly high, e.g. March 2015/ 2016.

3.4 Ocean-atmosphere emissions North of Svalbard

The aforementioned unexplained episode of increased CH_4 on ~25.08.2014 (Fig. 6) occurred at 80.4°N, 12.8°E, North of Svalbard. During this North Svalbard episode (NSE) wind speeds were ~7 m s^{-1} from a northerly direction. The absence of an excursion in the CO_2 mixing ratio at the same time suggests limited influence of wetlands (where a decrease would be expected) or anthropogenic emissions (where an increase would be expected). It is also noteworthy that the NSE is not predicted by the FLEXPART emissions, even though every other excursion >10 ppb during the entire measurement time series is predicted (Fig. S3). The FLEXPART footprint sensitivity shown in Figs. 8 and 9 for the RV Helmer Hanssen suggests that the measurements were highly sensitive to emissions close to the ship's location and over ocean areas north of Svalbard. Mixing ratios decreased as the measurements became less sensitive to this area after 12:00 on 26.08.2014 and then increased significantly once more on 27.08.2014 where measurements are likely to be influenced by wetland emissions in north east Russia, as also predicted by FLEXPART. During the NSE the Zeppelin Observatory was also highly sensitive to an area close to the measurement site, however in this case slightly to the south, mainly over land (North West Svalbard) while the sensitivity to land areas outside Svalbard appears similar (and very low) for both (Fig. S3).

During the NSE, measurements were sensitive to the relatively shallow Svalbard continental margin including the Hinlopen Strait (79.62°N, 18.78°E), Norskebanken (81.00°N, 14.00°E) and Yermak Plateaux (81.25°N, 5.00°E), (Fig. 8). This area is the site of the Hinlopen/Yermak Mega slide ~30 000 years before present (Winkelmann et al., 2006), where numerous bubble plumes (referred to as flares) emanating from the sea floor were recently discovered using echo-sounding and attributed to CH_4 venting (Geissler et al., 2016). We conclude that elevated mixing ratios on 25.08.2014 were the result of an ocean-atmosphere flux, based on the thorough analysis of over 2 years of measurement and model data, the presence of methane seepage, wind analysis and the footprint sensitivities shown in Figs. 8 and 9.

As described previously, the footprint sensitivity and the flux density of emissions within the sensitivity field yields the mixing ratio change at a receptor. We define the area of interest according to the active flare region described by Geissler et al. (2016) (Fig. 8C). There is a clear agreement between mean sensitivity to this active flare region and the atmospheric CH_4 mixing ratio

observed at the Helmer Hanssen (Fig. 9). Therefore, we calculate a flux for this area during this period (23-27.08.2014) by normalising the change in mixing ratio to the change in mean footprint sensitivity. The measurement points of lowest and highest CH_4 mixing ratios are well defined by the 25th and 75th percentiles, respectively (Fig. 9). To provide an estimate of the uncertainty in the flux we use a simple bootstrap: we generated new time series for CH_4 and mean sensitivity to the area of interest by resampling pairs of data points from the originals at random to create new time series of identical length and performed multiple repeats (n=10000) of the flux calculation. Accordingly, we attain a flux of 25.77±1.75 nmol $m^{-2}s^{-1}$, a total of 0.73±0.05 Gg yr^{-1} (assuming the flux only occurs in summer when the area is ice-free). We show the bootstrap distribution in Fig. S4.

There are two possible scenarios to explain why the NSE only appears to influence the RV Helmer Hanssen CH_4 time series on only one occasion: 1) A relatively high transient flux and 2) A transient, relatively high sensitivity to a small flux occurring in the area of interest. In order to evaluate this we repeat the calculation described above for all summer time periods (the area is largely ice bound outside of summer periods), i.e. we constrain the flux based on the difference in mixing ratios during time periods least sensitive and most sensitive to the area of interest, 'upwind' and 'downwind', respectively. For such a case, the estimate yields the maximum emission consistent with observations since it also neglects the influence of emissions outside the region of interest, while the true flux may be significantly lower or even negative. Pisso et al. (2016)~~.~~ d~~D~~escribe and evaluate this upwind-downwind methodology for constraining fluxes in more detail. We attained a maximum flux of 18.24 ± 2.79 nmol $m^{-2}s^{-1}$ based on all summer data, with the upwind-downwind analysis, slightly lower than the flux calculated for the NSE. This suggests that there was at least some increase in the CH_4 flux during the NSE relative to most periods (since the upwind-downwind calculation yields an absolute maximum). However, this difference is rather small, and Pisso et al. (2016) estimated a very similar flux threshold of 21.50 nmol $m^{-2}s^{-1}$ from an area around Svalbard covering 1644 km^2 where gas seeps have been observed. Accordingly, the area of interest North of Svalbard is unlikely to be unique in the context of the wider Arctic. Rather, that the meteorology at the time of the observation was unique in the context of the measurement time series, i.e. we obtained, over the short course of the episode, measurements highly sensitive to emissions over an active seep site, without sensitivity to land based emissions.

Extrapolating the flux densities in Table 1 to the known seep area, we attain a flux of up to 0.021±0.001 Tg ~~Y~~~~r~~yr^{-1}. This is obviously small compared to a global CH_4 budget of 550 Tg yr^{-1} (Saunois et al., 2016). Furthermore, only a change over time in the magnitude of a source will result in a climate forcing, suggesting only a very small influence of seafloor methane venting from this region on climate change at present.

The Ocean depth at the North Svalbard location was ~500 m. From this depth, it is very likely that CH_4 bubbles emanating from the sea floor will contain a gas phase composition almost identical to that of the atmosphere by the time they reach the surface due to diffusive exchange with dissolved gases in the water column. Any CH_4 flux from the ocean is therefore likely to be via diffusive flux of dissolved methane to the atmosphere. Since the ocean –atmosphere flux (F) is known it is also possible to estimate surface water concentrations (C_W) at the time of the episode by rearranging the sea-air exchange parameterisation of Wanninkhof et al. (2009), i.e.:

$$F = k\,(C_w - C_0) \rightarrow C_W = \frac{F}{k} + C_0 \quad , \qquad (2)$$

where k is the gas transfer velocity, and C_0 is the equilibrium dissolved CH_4 concentration at the surface. C_0 is given by

$$C_0 = exp\left\{ P_{CH4} - 415.2807 + 596.8104\left(\frac{100}{T_w}\right) + 379.2599\left[\ln\left(\frac{T_w}{100}\right)\right] - 62.0757\left(\frac{T_w}{100}\right) + S\left(-0.059160 + 0.032174\left(\frac{T_w}{100}\right) - 0.0048198\left(\frac{T_w}{100}\right)^2\right)\right\} , \qquad (3)$$

where P_{CH4} is the partial pressure of methane in the atmosphere, S is the salinity of spray above the ocean surface in ‰, which we assume is equivalent to surface water salinity, and T_w is the water temperature in Kelvins, from Wiesenburg and Guinasso Jr (1979). Equation 2 is valid for moist air, while we measure the dry air CH_4 mixing ratio ($X_{CH4,dry}$). To calculate P_{CH4} in the presence of water vapour we use

$$P_{CH4} = X_{CH4,dry} \times P_{atm}(1 - P_{H2O}) \ , \qquad (4)$$

where P_{atm} is the measured atmospheric pressure and P_{H2O} is the partial pressure of water, calculated according to Buck (1981) and accounting for measured relative humidity, $RH\%$:

$$P_{H2O} = 0.61121 \cdot \exp\left\{18.678 - \left(\frac{T_{air}}{234.5}\right)\left(\frac{T_{air}}{257.14+T_{air}}\right)\right\} \cdot \frac{RH\%}{100} \ , \qquad (5)$$

where T_{air} is the measured air temperature in °C. The gas transfer velocity in Eq. 2 is given by

$$k = 0.24 \times u_{10}^2 \left(\frac{Sc}{660}\right)^{-0.5}, \qquad (6)$$

where u_{10} is the wind velocity at 10 m and S_C is the Schmidt number, the non-dimensional ratio of gas diffusivity and water kinematic viscosity. We calculate S_C using the paramaterisation of Wanninkhof (2014):

$$S_C = 2101.2 - \left(131.54(T_w - 273.15)\right) + \left(4.4931(T_w - 273.15)\right)^2 - \left(0.08676(T_w - 273.15)\right)^3 + \left(0.00070663 \times (T_w - 273.15)\right)^4 . \qquad (7)$$

Finally, we correct for the difference in measurement height (22.4 m) and u_{10} using a power law dependence described by

$$u_{10} = u_{22.4} \times \left(\frac{10}{22.4}\right)^{0.11}, \qquad (8)$$

Equation 6 shows that CH_4 flux is proportional to the square of wind-speed while Eq. 7 demonstrates that water temperature also has a non-linear effect on the flux via the Schmidt number. Wind speed and water temperature are thus the two most important factors determining the ocean-atmosphere methane flux. We calculate uncertainties in Eq. 2 via a Monte Carlo approach by performing 10000 repeat calculations and incorporating normally distributed random noise (mean values of zero, standard deviations from observations) for wind speed, CH_4 atmospheric mixing ratios, and water temperatures. We use the bootstrap distribution in Fig. S4 for the uncertainty of the flux. We then calculate the final uncertainty in C_W from the distribution of the results from the Monte Carlo simulation.

During the NSE, we calculate that a dissolved CH_4 concentration of 555±297 nmol L^{-1} would have been required to generate the transient flux of 25.77±1.75 nmol m^{-2} s^{-1} given in Table 1. This concentration is higher than what was observed in surface waters over shallow (50-120m depth) seep sites West of Svalbard where Graves et al. (2015) report surface water CH_4

concentrations <52 nmol L^{-1}. ~~Silyakova et al. (submitted) report surface water CH_4 concentrations of <10 nmol L^{-1}.~~ ~~Very~~ Very high fluxes of CH_4 from sub seabed sources to the atmosphere have also been reported for the East Siberian Arctic Shelf (ESAS) (Shakhova et al., 2014), with flux values of ~70–450 nmol m^{-2} s^{-1} under stormy conditions with~~. The~~ surface water ~~concentration they report were of~~concentrations of the order of 450 nmol L^{-1}. However, the emissions reported for ESAS were over shallow water, and bubble dissolution, gas exchange, water column stratification, and microbial oxidation would significantly diminish CH_4 concentrations in the surface mixed layer above bubble emission sites in water depth >100 m (McGinnis et al., 2006;Mau et al., 2017;Graves et al., 2015~~)~~). Thus, there is an offset between the observed dissolved CH_4 concentrations and those previously observed over active marine seeps. Possible explanations for this offset include: 1) errors in the estimate of dissolved water CH_4 concentrations. 2) Additional (i.e. not seep related) sources of CH_4 in the water column. 3) Water conditions unique to this location and time allowing for higher dissolved CH_4 concentrations than normal in the region. 4) That the atmospheric CH_4 is at least partly from another source.

All of the above scenarios are possible to varying degrees. The Wanninkhof parameterisation (Eqs. 2-8) assumes emissions over a flat surface, which would be violated in the case of wind speeds at the time of the NSE of up to 7 ms^{-1}. Another source of error in the Cw estimation might be differences in wind speed over the seep site and measured at the RV Helmer Hanssen. Furthermore, while uncertainties in the required C_W are large, it should be noted that extreme values of dissolved CH_4 ~~methane~~ (e.g. >10^9 nmol ~~m^{-2}~~ ~~s~~L^{-1}) are obtainable from Eq. 2 for a net positive flux as wind speeds (and hence gas transfer velocity) approach zero. This nonlinear effect of wind speed is also evident in Fig. S5 which shows that the dissolved CH_4 required to produce the estimated ocean-atmosphere flux increases rapidly as the wind speed drops from 7 m s^{-1} to close to 1 m s^{-1}. I.e. the offset between previously observed dissolved CH_4 concentrations is small compared to what is obtainable via Eq. 2.

Other sources of marine CH_4 are also possible since the area had been covered by close drift ice only one week prior to our observations, and some open drift ice was still present in the area at the time of the measurements (Fig. S6). If any CH_4 is trapped under ice during winter, it may suddenly be released when the ice melts or is blown away. For example, Kort et al. (2012) report similar ocean-atmosphere CH_4 fluxes to those in this work of up to 2 mg d^{-1} m^{-2} (23 nmol m^{-2} s^{-1}) from observations of atmospheric CH_4 at Arctic sea-ice margins and ice leads. Meanwhile, Thornton et al. (2016) estimate that relatively high short lived CH_4 fluxes from the East Siberian Sea occur around melting ice, at 11.9 nmol m^{-2} s^{-1} (ice melt) vs 2.7 nmol m^{-2} s^{-1} (ice free).

~~Therefore, the reasonable agreement between the required C_W and previous studies shows that values for the fluxes in Table 1 are themselves reasonable and that the original assumption of an ocean-atmosphere flux is itself reasonable and consistent with observations. A~~A higher dissolved CH_4 concentration than observed West of Svalbard might also be due to rather low water temperatures at the North Svalbard site. We measured a water temperature of 0.7 °C for the area, vs 2-5°C for shallow waters west of Svalbard, (Silyakova et al., submitted) which might result in reduced CH_4 oxidation rates by methanotrophic bacteria, generally the main factor controlling CH_4 concentrations in the water column (Graves et al., 2015). Furthermore, lateral transport of CH_4 by ocean currents is also an important factor controlling dissolved concentrations and can be expected to vary by location (Steinle et al., 2015~~; Silyakova et al., submitted~~).

Formatted: Subscript

Finally, we cannot rule out other sources of CH_4 to the atmosphere, since there might be responsible for the observed excursion. This might be because of error in the footprint sensitivity field and or an extremely large flux in areas of low sensitivity. In summary therefore, there is no way to definitively prove, with available information that the NSE is due to ocean emissions, even if the evidence in favour is strong. Note that if there is no flux from the ocean, then the values in Table 1 can be considered as a constraint (maximum flux consistent with observations) on the CH_4 ocean atmosphere flux at this location. ~~, though it is possible that there is some discrepancy between wind speed measured at the ship and the source region itself. Very high fluxes of CH_4 from sub seabed sources to the atmosphere have been reported for the East Siberian Arctic Shelf (ESAS) (Shakhova et al., 2014), with flux values of ~70–450 nmol m^{-2} s^{-1} under stormy conditions. The surface water concentration they report were of the order of 450 nmol L^{-1}.~~

~~Therefore, the reasonable agreement between the required C_w and previous studies shows that values for the fluxes in Table 1 are themselves reasonable and that the original assumption of an ocean-atmosphere flux is itself reasonable and consistent with observations. A higher dissolved CH_4 concentration than observed West of Svalbard might be due to rather low water temperatures at the North Svalbard site. We measured a water temperature of -0.7 °C for the area, vs 2-5°C for shallow waters west of Svalbard, (Silyakova et al., submitted) which might result in reduced CH_4 oxidation rates by methanotrophic bacteria, generally the main factor controlling CH_4 concentrations in the water column (Graves et al., 2015). Furthermore, lateral transport of CH_4 by ocean currents is also an important factor controlling dissolved concentrations and can be expected to vary by location (Steinle et al., 2015; Silyakova et al., submitted).~~ Finally, ~~the area had been covered by close drift ice only one week prior to our observations, and some open drift ice was still present in the area at the time of the measurements (Fig. S6). If any CH_4 is trapped under ice during winter, it may suddenly be released when the ice melts or is blown away. For example, Kort et al. (2012) report similar ocean-atmosphere CH_4 fluxes to those in this work of up to 2 mg d^{-1} m^{-2} (23 nmol m^{-2} s^{-1}) from observations of atmospheric CH_4 at Arctic sea-ice margins and ice leads. Meanwhile, Thornton et al. (2016) estimate that relatively high short lived CH_4 fluxes from the East Siberian Sea occur around melting ice, at 11.9 nmol m^{-2} s^{-1} (ice melt) vs 2.7 nmol m^{-2} s^{-1} (ice free).~~

3.5 Offline trace gases and their potential use as gas hydrate tracers

While we present evidence of an observed ocean-atmosphere CH_4 flux in the previous section, the task of identifying and quantifying such fluxes would be considerably simplified if a unique tracer for oceanic CH_4 emissions were to exist. For this reason, we developed the new technique to analyse GH~~methane hydrate~~ composition described previously. On 23.05.2015 we took two sediment cores, CAGE 15-2 HH 911 GC and CAGE 15-2 HH 914 GC~~, were taken~~ from the seafloor at 76.11°N, 15.97°E and 76.11°N, 16.03°E, respectively (Fig.1 and Table 2). This area is noteworthy for the presence of conical hills or mounds (Serov et al., 2017) similar to terrestrial features called 'ping~~t~~os' (Mackay, 1998), with heights of ~10- 40 m and 100 m in diameter, and rising up to as near as 18 m to the sea surface. The core extracted at this location contained visible GH deposits, which we immediately sampled into an evacuated stainless steel flask for offline analysis of isotopes and trace gases.

Formatted: Subscript

The two GH samples contained 0.042 and 0.117 % ethane by mass (average 0.080 %), with the remaining volume consisting of methane (Table 2). All other hydrocarbons tested for (e.g. propane, butane) were below the detection limit, i.e. below ppt level (Miller et al., 2008), strong evidence of sample purity, since contamination with atmospheric air would lead to the presence of numerous other trace gases. We also determined isotopic ratios of –45.34 ±0.03 and –45.65 ±0.04‰ $\delta^{13}C$ in CH_4 vs V-PDB. The composition of gas contained in the same sediment cores as estimated by Serov et al., 2017 using the glass vial/ headspace method described in Sect. 2.4 is compared to our method in Table 2. For sample CAGE 15-2 HH 911 GC, Serov et al., 2017 report an average methane/ light hydrocarbon (ethane and propane) ratio (C1/(C2+C3)) an order of magnitude lower than observed using our methodology. Although the standard deviation was high, the maximum observed C1/(C2+C3) value was 460.06 vs our value, 2379.95. For sample CAGE 15-2 HH 914 GC, we observe a similar result; C1/(C2+C3) is higher using our methodology (1256.39) vs the headspace method (121.7±90.52, maximum 239.38). There may be several reasons for these discrepancies, as outlined in Sect. 2.4.

The relationship between hydrocarbon composition and isotopic composition can be used to define whether natural gas from a hydrocarbon seep is of thermogenic (cracking of hydrocarbons below the Earth's surface) or of biogenic origin (Bernard et al., 1976;Smith et al., 2014;Faramawy et al., 2016). Thermogenic natural gas exhibits C1/ (C2+C3) <1000 and $\delta^{13}C$ in CH_4 V-PDB > -50‰., whereas biogenic gas exhibits C1/ (C2+C3)>200 and $\delta^{13}C$ in CH_4 V-PDB < -50‰. Samples between these ranges are of mixed origin. Thus, based on the values shown in Table 2 (and other core samples around the same location), Serov et al. (2017) identify the gas contained in the sediments as unambiguously thermogenic in origin. However, the gas composition of the hydrates within the gravity cores determined using our methodology points to a biogenic or more mixed origin, since the C2+C3 fraction is rather low. Furthermore, hydrates are typically enriched in C2 and C3 hydrocarbons compared to the seep gas from which they emanate due to molecular fractionation (Sloan Jr, 1998), suggesting a lower C2+C3 fraction, and a lower thermogenic gas contribution in the sediments, than reported by (Serov et al., 2017). Our results therefore demonstrate, at the very least, the need for a harmonised technique for the analysis of natural gas from sediments, since the different methodologies used here indicate different sediment histories.

The C1/(C2+C3) ratios for the hydrate samples are close to those of the ambient atmosphere in the Arctic. For air samples collected in summer 2014, summer and autumn 2015 we obtain C1/(C2+C3) ratios of 2119.4, 2131.31, and 1467.21, respectively. The range over all values was from a minimum of 1230.39 to a maximum of 2526.17. We observed higher ratios in winter when photochemistry is slower and there is less oxidation of the relatively short-lived ethane/ propane compared to CH_4. We therefore expect ratios lower than 2526.31 in winter.

The background variations in C1/(C2+C3) ratios show that ethane is not a unique tracer for emissions to the atmosphere from hydrates of biogenic or mixed origin, i.e. additional information is required to quantify hydrate methane emission to the atmosphere. For example, using the summer 2014 data, a large enhancement in the CH_4 mixing ratio due to hydrate emissions reaching the atmosphere of 100 ppb would perturb the atmospheric C1/(C2+C3) ratio from 2131.31 to 2007.54, which would be detectable, but is well within the normal variation of the background ambient levels. Thermogenic hydrate emissions to the atmosphere meanwhile would produce larger variations. Using a C1/(C2+C3) ratio for gas hydrates ~~od~~ of 121.7 from Table 2,

we attain a change in atmospheric C1/(C2+C3) ratio from 2131.31 to 1109.93 for a 100 ppb increase in CH_4 mixing ratio due to gas hydrates, just outside the range of observed ambient values in this study. Thus the C1/(C2+C3) ratio might be useful to identify CH_4 reaching the atmosphere from thermogenic seeps and hydrates, however this would only be applicable in extreme cases, since we did not observe excursions from the CH_4 baseline mixing ratio of the order of 100 ppb away from coastline settlements. A more realistic methane enhancement of 30 ppb might result in a change in the C1/(C2+C3) ratio from 2131.31 to 1557.19, falling well within the observed background variation. Importantly however, these simple calculations neglect the influence of bacterial oxidation in the water column. The capacity of microbes to remove dissolved CH_4 from the water column may be considerable and methanotrophic bacteria are already thought to heavily mitigate ocean-atmosphere methane emissions (Crespo-Medina et al., 2014). For example, following the Deep Water Horizon drilling rig explosion on April 20th, 2010 bacteria removed almost all of the methane released to the water column at a rate of 5900 nmol L^{-1} day^{-1} (Crespo-Medina et al., 2014). ~~Meanwhile, nutrient upwelling over seep sites at Prins Karls Forland may support sufficient biomass to cause reductions in atmospheric CO_2 mixing ratios to more than offset any warming due to CH_4 emission from the seeps (Pohlman et al., 2017).~~

The effect of bacterial oxidation on ethane and even propane emanating from the ocean is even less clear. However, ethanotrophic and propanotrophic bacteria are thought to be extant (Kinnaman et al., 2007), and many methanotrophes are also observed to cometabolise heavier hydrocarbons (Berthe-Corti and Fetzner, 2002). Kinnaman et al. (2007) also observed preferential metabolism of C2-C4 hydrocarbons over CH_4 in incubated hydrocarbon rich sediments, while Valentine et al. (2010) observed that propanotrophic and ethanotrophic bacteria were responsible for 70% of the oxygen depletion due to microbial activity in the pollution plume from the 2010 Deep Water Horizon drilling rig explosion in the Gulf of Mexico. Thus, there is considerable uncertainty as to what effect co-release of ethane or propane from hydrates into the water column will have on the atmosphere, making ethane an unreliable tracer for ocean-atmosphere CH_4 emissions.

Changes in atmospheric $\delta^{13}C$ in CH_4 vs V-PDB are similarly unreliable as a marker for ocean-atmosphere CH_4 from subsea seeps because these are so close to ambient atmospheric background isotopic ratios. For example, using the values determined from the hydrates in this study in Table 2 and a background average from the offline samples of -47.12 ‰, an increase of the atmospheric CH_4 mixing ratio of 40 ppb is needed to perturb the background ratio by more than the isotope analysis method precision, which averages 0.04‰. For a value of three times the precision, close to a 100 ppb increase in methane due to hydrate emission would be required. The isotope analysis technique in this study is state-of-the-art, compared to a typical precision for $\delta^{13}C$ in methane of 0.05‰ (Rice et al., 2001;Miller et al., 2002), but is only capable of detecting changes in $\delta^{13}C$ resulting from relatively large changes in CH_4 mixing ratios due to subsea emissions, i.e., larger than observed in our methane time series. Furthermore, as with ethane and propane, the isotopic ratio lacks specificity. $\delta^{13}C$ in CH_4 for hydrates ranges from ≈-70 to -30 ‰ vs V-PDB for biogenic and thermogenic hydrate types, respectively. This range overlaps with that of other sources, e.g. natural gas leaks or landfill emissions. Thus, $\delta^{13}C$ in CH_4 vs V-PDB is strongly indicative of whether a source is biogenic or thermogenic in origin (Saunois et al., 2016) but cannot be used to distinguish between the reservoirs in which CH_4 is stored, i.e., whether CH_4 has been released from gas hydrates or subsea hydrocarbon seeps or land based hydrocarbon seeps.

While both isotopic ratios and the C1/(C2+C3) ratio are not unique tracers, and even though subsea sources are not expected to perturb background atmospheric isotopic and light hydrocarbon composition except at relatively high emission rates, they can nevertheless be used as part of an integrated approach to constrain CH_4 sources, e.g., in multi-species inverse modelling (Thompson et al., 2018). Furthermore, both parameters are of considerable use in the analysis of global and regional trends in CH_4 (e.g. Dalsøren et al., 2018;Fisher et al., 2011). The main limitation revealed by this study is practicality for constraining the relatively small ocean-atmosphere fluxes. The highly sensitive techniques used here require offline analysis of flask samples (see Sect. 2.3) in order to yield high analytical precision. Consequently, it is not feasible to obtain samples at every possible location or point in time. The collection of samples for analysis of isotopic and light hydrocarbon composition from subsea sources very likely requires a priori knowledge of a seep site location, and even then, there is no guarantee that measurements are highly sensitive to the location of the research vessel. However, with enough samples collected at a known seep site, changes in the atmospheric isotopic composition and C1/(C2+C3) ratio could be used to quantify a flux.

4 Conclusions

We have presented long term, high-resolution CH_4 atmospheric mixing ratios from measurements at the Zeppelin Mountain Observatory and the RV Helmer Hanssen. We have also analysed additional trace gases (ethane, propane, and CO_2) and isotopic composition in offline samples collected at the Helmer Hanssen, and modelled air mass trajectories with FLEXPART. According to the data from Zeppelin, the trend of increasing CH_4 mixing ratio since 2005 continued in 2017, increasing in average ca 8 ppb after 2010. Atmospheric CH_4 mixing ratios in the Arctic are highly variable with baseline excursions of ~30 ppb being commonplace. With our dataset we are able to attribute all but one of the observed large excursions (>10 pbb) in background CH_4 observed over different locations of the Arctic Ocean in June 2014- December 2016 to land based sources (wetlands, anthropogenic emissions, biomass burning) by combining data from emission inventories and an atmospheric transport model. We also observe high correlations between models and observations on a monthly basis (up to R^2=0.8). In this context the large excursion in CH_4 occurring during measurements along the coast of North Svalbard in August 2014 is unique and there is good evidence that we observed an ocean-atmosphere methane flux of up to 26 nmol $m^{-2}s^{-1}$. This result agrees well with previous constraints on ocean-atmosphere fluxes (Myhre et al., 2016;Pisso et al., 2016), and demonstrates the importance of long term measurements in the region to assess in-depth processes, i.e. the excursion from the background CH_4 mixing ratio is only unique in the broader context of a time series where every other excursion is well explained.

We also found that neither co-emitted light hydrocarbons (ethane/ propane) nor the $\delta^{13}C$ isotopic ratio of CH_4 are unique tracers for ocean atmosphere emission from subsea seeps and hydrates. Further demonstrating that identifying ocean atmosphere CH_4 emission sources is only possible via careful analysis of measurement data, combining both ocean and atmospheric measurements and analysis. Nevertheless, with a priori knowledge of the location of an ocean source, light hydrocarbon and isotopic composition may be useful for the quantification of fluxes if the flux is large enough. That is, atmospheric $\delta^{13}C$-CH_4

and C1/(C2+C3) ratios are potentially more useful for quantification of fluxes from strong, known sources rather than the identification of new or potentially very small sources.

Finally, the fluxes we (and others) determined for sub-sea seep and hydrate derived ocean-atmosphere CH_4 emissions are trivial compared to the global CH_4 budget, even if extrapolated to much larger areas. Nevertheless, the Arctic is changing rapidly in response to climate change, and changes in the flux over time could contribute to future warming, thus our results are a baseline against which future ocean atmosphere CH_4 emissions can be compared.

Data Availability

All atmospheric data from Zeppelin and RV Helmer Hanssen are publicly available on the EBAS database (http://ebas.nilu.no). The harmonised dataset of historic CH_4 mixing ratio measurements is archived in the ICOS Carbon portal (ICOS, 2018).

Author contributions

Trace gas measurements Helmer Hanssen: O.H., B.F., P.J., A. Silyakova, S.V., J.M.; Methane measurements Zeppelin: O.H., N.S., C.L.M.; Trend calculation methane at Zeppelin: T.S., C.L.M.; Development of gas hydrate sampling technique: N.S.; FLEXPART model runs: I.P., A. Stohl; Emissions: S.E, A. Stohl; Isotopic analysis: E.G.N., D.L, R.F.; Data analysis trace gases at Helmer Hanssen and flux calculations: S.P.; Manuscript writing: S.P; Review of manuscript: All

Competing interests

The authors declare no competing interests

Acknowledgements

SOCA- *Signals from the Arctic OCean to the Atmosphere*, NILU's strategic initiative (SIS) project funded by the Research Council of Norway. MOCA- *Methane Emissions from the Arctic OCean to the Atmosphere: Present and Future Climate Effects* was funded by the Research Council of Norway, grant no.225814. CAGE – Centre for Arctic Gas Hydrate, Environment and Climate research work was supported by the Research Council of Norway through its Centres of Excellence funding scheme grant no. 223259.

References

Bernard, B. B., Brooks, J. M., and Sackett, W. M.: Natural gas seepage in the Gulf of Mexico, Earth and Planetary Science Letters, 31, 48-54, 1976.

Berthe-Corti, L., and Fetzner, S.: Bacterial Metabolism of n-Alkanes and Ammonia under Oxic, Suboxic and Anoxic Conditions, Engineering in Life Sciences, 22, 299-336, 2002.

Bousquet, P., Ringeval, B., Pison, I., Dlugokencky, E., Brunke, E.-G., Carouge, C., Chevallier, F., Fortems-Cheiney, A., Frankenberg, C., and Hauglustaine, D.: Source attribution of the changes in atmospheric methane for 2006–2008, Atmospheric Chemistry and Physics, 11, 3689-3700, 2011.

Buck, A. L.: New equations for computing vapor pressure and enhancement factor, Journal of Applied Meteorology, 20, 1527-1532, 1981.

Chylek, P., Folland, C. K., Lesins, G., Dubey, M. K., and Wang, M.: Arctic air temperature change amplification and the Atlantic Multidecadal Oscillation, Geophysical Research Letters, 36, 2009.

Cohen, J., Screen, J. A., Furtado, J. C., Barlow, M., Whittleston, D., Coumou, D., Francis, J., Dethloff, K., Entekhabi, D., and Overland, J.: Recent Arctic amplification and extreme mid-latitude weather, Nature geoscience, 7, 627-637, 2014.

Crespo-Medina, M., Meile, C., Hunter, K., Diercks, A., Asper, V., Orphan, V., Tavormina, P., Nigro, L., Battles, J., and Chanton, J.: The rise and fall of methanotrophy following a deepwater oil-well blowout, Nature Geoscience, 7, 423-427, 2014.

Dalsøren, S. B., Myhre, C. L., Myhre, G., Gomez-Pelaez, A. J., Søvde, O. A., Isaksen, I. S., Weiss, R. F., and Harth, C. M.: Atmospheric methane evolution the last 40 years, Atmospheric Chemistry and Physics, 16, 3099-3126, 2016.

Dalsøren, S. B., Myhre, G., Hodnebrog, Ø., Myhre, C. L., Stohl, A., Pisso, I., Schwietzke, S., Höglund-Isaksson, L., Helmig, D., and Reimann, S.: Discrepancy between simulated and observed ethane and propane levels explained by underestimated fossil emissions, Nature Geoscience, 11, 178, 2018.

Dlugokencky, E., Bruhwiler, L., White, J., Emmons, L., Novelli, P. C., Montzka, S. A., Masarie, K. A., Lang, P. M., Crotwell, A., and Miller, J. B.: Observational constraints on recent increases in the atmospheric CH4 burden, Geophysical Research Letters, 36, 2009.

ECLIPSE V5a global emission fields, http://www.iiasa.ac.at/web/home/research/researchPrograms/air/ECLIPSEv5a.html, accessed June 15th, 2018.

Etminan, M., Myhre, G., Highwood, E., and Shine, K.: Radiative forcing of carbon dioxide, methane, and nitrous oxide: A significant revision of the methane radiative forcing, Geophysical Research Letters, 43, 2016.

Faramawy, S., Zaki, T., and Sakr, A.-E.: Natural gas origin, composition, and processing: A review, Journal of Natural Gas Science and Engineering, 34, 34-54, 2016.

Fisher, R. E., Sriskantharajah, S., Lowry, D., Lanoisellé, M., Fowler, C., James, R., Hermansen, O., Lund Myhre, C., Stohl, A., and Greinert, J.: Arctic methane sources: Isotopic evidence for atmospheric inputs, Geophysical Research Letters, 38, 2011.

Geissler, W. H., Gebhardt, A. C., Gross, F., Wollenburg, J., Jensen, L., Schmidt-Aursch, M. C., Krastel, S., Elger, J., and Osti, G.: Arctic megaslide at presumed rest, Scientific Reports, 6, 2016.

Graves, C. A., Steinle, L., Rehder, G., Niemann, H., Connelly, D. P., Lowry, D., Fisher, R. E., Stott, A. W., Sahling, H., and James, R. H.: Fluxes and fate of dissolved methane released at the seafloor at the landward limit of the gas hydrate stability zone offshore western Svalbard, Journal of Geophysical Research: Oceans, 120, 6185-6201, 2015.

Hartmann, D. L., A.M.G. Klein Tank, M. Rusticucci, L.V. Alexander, S. Brönnimann, Y. Charabi, F.J. Dentener, E.J. Dlugokencky, D.R. Easterling, A. Kaplan, B.J. Soden, P.W. Thorne, Wild, M., and Zhai, P. M.: Observations: Atmosphere and Surface. In: Climate Change 2013: The Physical Science Basis. Contribution of Working Group I to the Fifth Assessment Report of the Intergovernmental Panel on Climate Change, Cambridge University Press, Cambridge, United Kingdom and New York, NY, USA, 2013.

Hayhoe, K., Kheshgi, H. S., Jain, A. K., and Wuebbles, D. J.: Substitution of natural gas for coal: climatic effects of utility sector emissions, Climatic Change, 54, 107-139, 2002.

Helmig, D., Rossabi, S., Hueber, J., Tans, P., Montzka, S. A., Masarie, K., Thoning, K., Plass-Duelmer, C., Claude, A., and Carpenter, L. J.: Reversal of global atmospheric ethane and propane trends largely due to US oil and natural gas production, Nature Geoscience, 9, 490, 2016.

Hu, F. S., Higuera, P. E., Duffy, P., Chipman, M. L., Rocha, A. V., Young, A. M., Kelly, R., and Dietze, M. C.: Arctic tundra fires: natural variability and responses to climate change, Frontiers in Ecology and the Environment, 13, 369-377, 2015.

Höglund-Isaksson, L.: Bottom-up simulations of methane and ethane emissions from global oil and gas systems 1980 to 2012, Environmental Research Letters, 12, 2017.

Jakobsson, M., Mayer, L., Coakley, B., Dowdeswell, J. A., Forbes, S., Fridman, B., Hodnesdal, H., Noormets, R., Pedersen, R., and Rebesco, M.: The international bathymetric chart of the Arctic Ocean (IBCAO) version 3.0, Geophysical Research Letters, 39, 2012.

ICOS Carbon Portal, Integrated Non-CO2 Observing System (INGOS), & Bergamaschi, P. (2018, January 23). Ensemble of inverse modelling results of European CH4 emissions during 2006-2012. ICOS ERIC - Carbon Portal. https://doi.org/10.18160/vnx5-qxcb, 2018.

IPCC, 2013: Climate Change 2013: The Physical Science Basis. Contribution of Working Group I to the Fifth Assessment Report of the Intergovernmental Panel on Climate Change [Stocker, T.F., D. Qin, G.-K. Plattner, M. Tignor, S.K. Allen, J. Boschung, A. Nauels, Y. Xia, V. Bex and P.M. Midgley (eds.)]. Cambridge University Press, Cambridge, United Kingdom and New York, NY, USA, 1535 pp

Kinnaman, F. S., Valentine, D. L., and Tyler, S. C.: Carbon and hydrogen isotope fractionation associated with the aerobic microbial oxidation of methane, ethane, propane and butane, Geochimica et Cosmochimica Acta, 71, 271-283, 2007.

Kirschke, S., Bousquet, P., Ciais, P., Saunois, M., Canadell, J. G., Dlugokencky, E. J., Bergamaschi, P., Bergmann, D., Blake, D. R., and Bruhwiler, L.: Three decades of global methane sources and sinks, Nature Geoscience, 6, 813-823, 2013.

Kort, E., Wofsy, S., Daube, B., Diao, M., Elkins, J., Gao, R., Hintsa, E., Hurst, D., Jimenez, R., and Moore, F.: Atmospheric observations of Arctic Ocean methane emissions up to 82 north, Nature Geoscience, 5, 318, 2012.

Kretschmer, K., Biastoch, A., Rüpke, L., and Burwicz, E.: Modeling the fate of methane hydrates under global warming, Global Biogeochemical Cycles, 29, 610-625, 2015.

Kvenvolden, K. A.: Methane hydrate—a major reservoir of carbon in the shallow geosphere?, Chemical geology, 71, 41-51, 1988.

LPX-Bern-DYPTOP-CH4, LPX-Bern: Simulated dynamics of global wetlands and peatlands with associated CH4 fluxes, data set available at www.climate.unibe.ch, accessed June 15th, 2018.

Mackay, J.: Pingo growth and collapse, Tuktoyaktuk Peninsula area, western Arctic coast, Canada: A long-term field study, Géographie physique et Quaternaire, 52, 271-323, 1998.

Marín-Moreno, H., Giustiniani, M., Tinivella, U., and Piñero, E.: The challenges of quantifying the carbon stored in Arctic marine gas hydrate, Marine and Petroleum Geology, 71, 76-82, 2016.

Mau, S., Römer, M., Torres, M. E., Bussmann, I., Pape, T., Damm, E., Geprägs, P., Wintersteller, P., Hsu, C.-W., and Loher, M.: Widespread methane seepage along the continental margin off Svalbard-from Bjørnøya to Kongsfjorden, Scientific reports, 7, 42997, 2017.

McGinnis, D. F., Greinert, J., Artemov, Y., Beaubien, S., and Wüest, A.: Fate of rising methane bubbles in stratified waters: How much methane reaches the atmosphere?, Journal of Geophysical Research: Oceans, 111, 2006.

Miller, B. R., Weiss, R. F., Salameh, P. K., Tanhua, T., Greally, B. R., Mühle, J., and Simmonds, P. G.: Medusa: A sample preconcentration and GC/MS detector system for in situ measurements of atmospheric trace halocarbons, hydrocarbons, and sulfur compounds, Analytical Chemistry, 80, 1536-1545, 2008.

Miller, J. B., Mack, K. A., Dissly, R., White, J. W., Dlugokencky, E. J., and Tans, P. P.: Development of analytical methods and measurements of 13C/12C in atmospheric CH4 from the NOAA Climate Monitoring and Diagnostics Laboratory Global Air Sampling Network, Journal of Geophysical Research: Atmospheres, 107, 2002.

Myhre, C. L., Ferré, B., Platt, S. M., Silyakova, A., Hermansen, O., Allen, G., Pisso, I., Schmidbauer, N., Stohl, A., and Pitt, J.: Extensive release of methane from Arctic seabed west of Svalbard during summer 2014 does not influence the atmosphere, Geophysical Research Letters, 43, 4624-4631, 2016.

NILU-FLEXTRA Back trajectories, https://www.nilu.no/projects/ccc/trajectories/, accessed 04.06.2018: https://www.nilu.no/projects/ccc/trajectories/) 2018.

Nisbet, E., Dlugokencky, E., Manning, M., Lowry, D., Fisher, R., France, J., Michel, S., Miller, J., White, J., and Vaughn, B.: Rising atmospheric methane: 2007–2014 growth and isotopic shift, Global Biogeochemical Cycles, 30, 1356-1370, 2016.

Pisso, I., Myhre, C. L., Platt, S., Eckhardt, S., Hermansen, O., Schmidbauer, N., Mienert, J., Vadakkepuliyambatta, S., Bauguitte, S., and Pitt, J.: Constraints on oceanic methane emissions west of Svalbard from atmospheric in situ measurements and Lagrangian transport modeling, Journal of Geophysical Research: Atmospheres, 121, 2016.

Pohlman, J. W., Greinert, J., Ruppel, C., Silyakova, A., Vielstädte, L., Casso, M., Mienert, J., and Bünz, S.: Enhanced CO2 uptake at a shallow Arctic Ocean seep field overwhelms the positive warming potential of emitted methane, Proceedings of the National Academy of Sciences, 201618926, 2017.

Prinn, R. G., Weiss, R. F., Krummel, P. B., O'Doherty, S., Fraser, P., Muhle, J., Reimann, S., Vollmer, M., Simmonds, P. G., and Malone, M.: The ALE/GAGE/AGAGE Network, Massachusetts Institute of Technology, Cambridge, MA (USA);, 2008.

Randerson, J. T., van der Werf, G., Giglio, L., Collatz, G. J., and Kasibhatla., P. S.: Global Fire Emissions Database, Version 4.1 (GFEDv4). ORNL DAAC, Oak Ridge, Tennessee, USA. https://doi.org/10.3334/ORNLDAAC/1293, 2017.

Reeburgh, W. S.: Oceanic methane biogeochemistry, Chemical reviews, 107, 486-513, 2007.

Formatted: EndNote Bibliography

Rice, A., Gotoh, A., Ajie, H., and Tyler, S.: High-precision continuous-flow measurement of δ13C and δD of atmospheric CH4, Analytical Chemistry, 73, 4104-4110, 2001.

Rigby, M., Prinn, R. G., Fraser, P. J., Simmonds, P. G., Langenfelds, R., Huang, J., Cunnold, D. M., Steele, L. P., Krummel, P. B., and Weiss, R. F.: Renewed growth of atmospheric methane, Geophysical research letters, 35, 2008.

Saunois, M., Bousquet, P., Poulter, B., Peregon, A., Ciais, P., Canadell, J. G., Dlugokencky, E. J., Etiope, G., Bastviken, D., and Houweling, S.: The global methane budget 2000-2012, Earth System Science Data, 8, 697, 2016.

Serov, P., Vadakkepuliyambatta, S., Mienert, J., Patton, H., Portnov, A., Silyakova, A., Panieri, G., Carroll, M. L., Carroll, J., and Andreassen, K.: Postglacial response of Arctic Ocean gas hydrates to climatic amelioration, Proceedings of the National Academy of Sciences, 201619288, 2017.

Shakhova, N., Semiletov, I., Leifer, I., Sergienko, V., Salyuk, A., Kosmach, D., Chernykh, D., Stubbs, C., Nicolsky, D., and Tumskoy, V.: Ebullition and storm-induced methane release from the East Siberian Arctic Shelf, Nature Geoscience, 7, 64-70, 2014.

Silyakova, A., Jansson, P., Serov, P., Ferre, B., Pavlov, A., Hattermann, T., Graves, C. A., Platt, S. M., Myhre, C. L., Gründger, F., and Niemann, H.: Controls of methane transport through the water column above a shallow shelf seep area west of Svalbard, submitted to JGR Oceans, submitted.

Simmonds, P., Manning, A., Cunnold, D., McCulloch, A., O'Doherty, S., Derwent, R., Krummel, P., Fraser, P., Dunse, B., and Porter, L.: Global trends, seasonal cycles, and European emissions of dichloromethane, trichloroethene, and tetrachloroethene from the AGAGE observations at Mace Head, Ireland, and Cape Grim, Tasmania, Journal of Geophysical Research: Atmospheres, 111, 2006.

Sloan Jr, E. D.: Clathrate Hydrates of Natural Gases, revised and expanded, Crc Press, 1998.

Smith, A. J., Mienert, J., Bünz, S., and Greinert, J.: Thermogenic methane injection via bubble transport into the upper Arctic Ocean from the hydrate-charged Vestnesa Ridge, Svalbard, Geochemistry, Geophysics, Geosystems, 15, 1945-1959, 2014.

Spahni, R., Wania, R., Neef, L., Weele, M. v., Pison, I., Bousquet, P., Frankenberg, C., Foster, P., Joos, F., and Prentice, I.: Constraining global methane emissions and uptake by ecosystems, Biogeosciences, 8, 1643-1665, 2011.

Stocker, B., Spahni, R., and Joos, F.: DYPTOP: a cost-efficient TOPMODEL implementation to simulate sub-grid spatio-temporal dynamics of global wetlands and peatlands, Geoscientific Model Development, 7, 3089-3110, 2014.

Stohl, A., Forster, C., Frank, A., Seibert, P., and Wotawa, G.: The Lagrangian particle dispersion model FLEXPART version 6.2, Atmospheric Chemistry and Physics, 5, 2461-2474, 2005.

Stohl, A., Berg, T., Burkhart, J., Fjæraa, A., Forster, C., Herber, A., Hov, Ø., Lunder, C., McMillan, W., and Oltmans, S.: Arctic smoke–record high air pollution levels in the European Arctic due to agricultural fires in Eastern Europe in spring 2006, Atmospheric Chemistry and Physics, 7, 511-534, 2007.

Stohl, A., Klimont, Z., Eckhardt, S., Kupiainen, K., Shevchenko, V. P., Kopeikin, V., and Novigatsky, A.: Black carbon in the Arctic: the underestimated role of gas flaring and residential combustion emissions, Atmospheric Chemistry and Physics, 13, 8833-8855, 2013.

Stohl, A., Aamaas, B., Amann, M., Baker, L., Bellouin, N., Berntsen, T. K., Boucher, O., Cherian, R., Collins, W., and Daskalakis, N.: Evaluating the climate and air quality impacts of short-lived pollutants, Atmospheric Chemistry and Physics, 15, 10529-10566, 2015.

Taylor, K. E.: Summarizing multiple aspects of model performance in a single diagram, Journal of Geophysical Research: Atmospheres, 106, 7183-7192, 2001.

Thompson, R. L., Sasakawa, M., Machida, T., Aalto, T., Worthy, D., Lavric, J. V., Lund Myhre, C., and Stohl, A.: Methane fluxes in the high northern latitudes for 2005–2013 estimated using a Bayesian atmospheric inversion, Atmospheric Chemistry and Physics, 17, 3553-3572, 2017.

The EBAS database, ebas.nilu.no, accessed June 15th, 2018.

Thornton, B. F., Geibel, M. C., Crill, P. M., Humborg, C., and Mörth, C. M.: Methane fluxes from the sea to the atmosphere across the Siberian shelf seas, Geophysical Research Letters, 43, 5869-5877, 2016.

United Nations Framework Convention on Climate Change (UNFCCC), http://di.unfccc.int/detailed_data_by_party, accessed 24.05.2018, 2018.

Valentine, D. L., Kessler, J. D., Redmond, M. C., Mendes, S. D., Heintz, M. B., Farwell, C., Hu, L., Kinnaman, F. S., Yvon-Lewis, S., and Du, M.: Propane respiration jump-starts microbial response to a deep oil spill, Science, 330, 208-211, 2010.

Wallmann, K., Riedel, M., Hong, W.-L., Patton, H., Hubbard, A., Pape, T., Hsu, C., Schmidt, C., Johnson, J. E., and Torres, M.: Gas hydrate dissociation off Svalbard induced by isostatic rebound rather than global warming, Nature communications, 9, 83, 2018.

Wanninkhof, R., Asher, W. E., Ho, D. T., Sweeney, C., and McGillis, W. R.: Advances in quantifying air-sea gas exchange and environmental forcing, 2009.

Wanninkhof, R.: Relationship between wind speed and gas exchange over the ocean revisited, Limnology and Oceanography: Methods, 12, 351-362, 2014.

Westbrook, G. K., Thatcher, K. E., Rohling, E. J., Piotrowski, A. M., Pälike, H., Osborne, A. H., Nisbet, E. G., Minshull, T. A., Lanoisellé, M., and James, R. H.: Escape of methane gas from the seabed along the West Spitsbergen continental margin, Geophysical Research Letters, 36, 2009.

Wiesenburg, D. A., and Guinasso Jr, N. L.: Equilibrium solubilities of methane, carbon monoxide, and hydrogen in water and sea water, Journal of Chemical and Engineering Data, 24, 356-360, 1979.

Winkelmann, D., Jokat, W., Niessen, F., Stein, R., and Winkler, A.: Age and extent of the Yermak Slide north of Spitsbergen, Arctic Ocean, Geochemistry, Geophysics, Geosystems, 7, 2006.

WMO: World Meteorological Office (WMO) Statement on the state of the global climate in 2017, https://library.wmo.int/opac/doc_num.php?explnum_id=4453, accessed June 15th 2018, 2017.

Worden, J. R., Bloom, A. A., Pandey, S., Jiang, Z., Worden, H. M., Walker, T. W., Houweling, S., and Röckmann, T.: Reduced biomass burning emissions reconcile conflicting estimates of the post-2006 atmospheric methane budget, Nature communications, 8, 2227, 2017.

Yttri, K. E., Lund Myhre, C., Eckhardt, S., Fiebig, M., Dye, C., Hirdman, D., Ström, J., Klimont, Z., and Stohl, A.: Quantifying black carbon from biomass burning by means of levoglucosan–a one-year time series at the Arctic observatory Zeppelin, Atmospheric Chemistry and Physics, 14, 6427-6442, 2014.

Aman, A. A. and Bman, B. B.: The test article, J. Sci. Res., 12, 135–147, doi:10.1234/56789, 2015.

Aman, A. A., Cman, C., and Bman, B. B.: More test articles, J. Adv. Res., 35, 13–28, doi:10.2345/67890, 2014.

Table 1: Maximum fluxes of methane from the ocean at the North Svalbard location determined from summer data and the flux during the episode of high CH_4 mixing ratios

Summertime (maximum from constraint)		**Flux during episode**	
Flux density [nmol $m^{-2}s^{-1}$]	**Total emission [Gg yr^{-1}]**	**Flux density [nmol $m^{-2}s^{-1}$]**	**Total emission [Gg yr^{-1}]**
18.24± 2.79	0.52±0.08	25.77±1.75	0.73±0.05

Table 2: Gas composition of hydrate and gravity core samples by mass from the Storfjordrenna hydrate pingo area according to this work and to (Serov et al., 2017)

	CAGE 15-2 HH 911 GC (15.97°E/76.11°N)		CAGE 15-2 HH 914 GC (16.03°E/76.11°N)	
	This work	Serov et al., 2017	This work	Serov et al., 2017
C1/ (C2+C3)	2379.95	164.51±173.27	853.70	121.70±90.42
δ^{13}C V-PDB	–45.34 ±0.03	-48.4	–45.65 ±0.04	-44.7

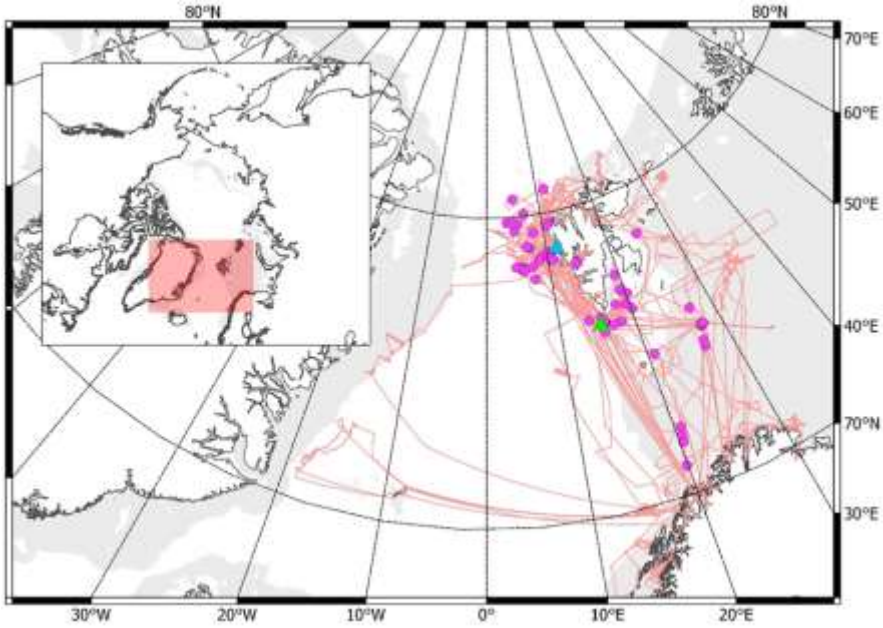

Figure 1: Route of the RV Helmer Hanssen (pink line) in 2014-2016, locations of offline flask samples (violet dots), the Zeppelin Observatory (blue triangle), and the location from which hydrates were collected from the seafloor (green triangle). Light grey shows areas of shallow ocean (100-400 m deep) according to the International Bathymetric Chart of the Arctic Ocean , IBCAO (Jakobsson et al., 2012). Sampling locations included much of the Svalbard coast, the Barents Sea, the Norwegian coast and waters off Greenland. The inset shows the global location of the measurements, with the area of the larger map shown by the shaded region.

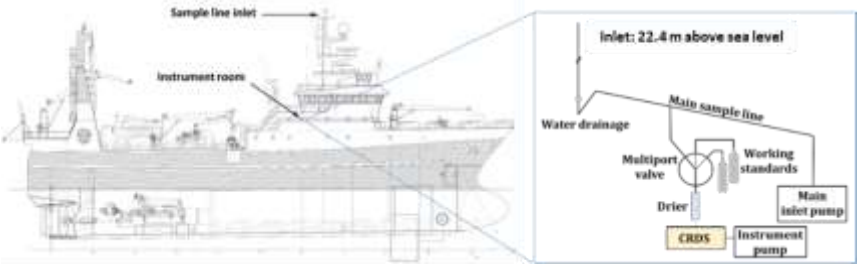

Figure 2: Schematic of the RV Helmer Hanssen showing the location of the sample inlet (to scale) and schematic of instrument room (not to scale).

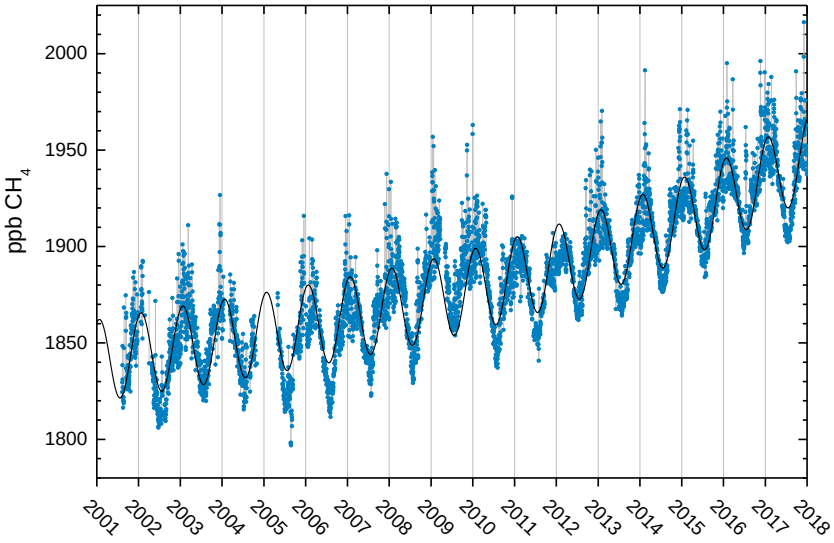

Figure 3: Observations of daily averaged CH_4 mixing ratio for the period 2001-2017 at the Zeppelin Observatory. The blue dots are daily mean mixing ratios in ppb, and the black solid line is the empirically fitted CH_4 mixing ratio (Eq. 1).

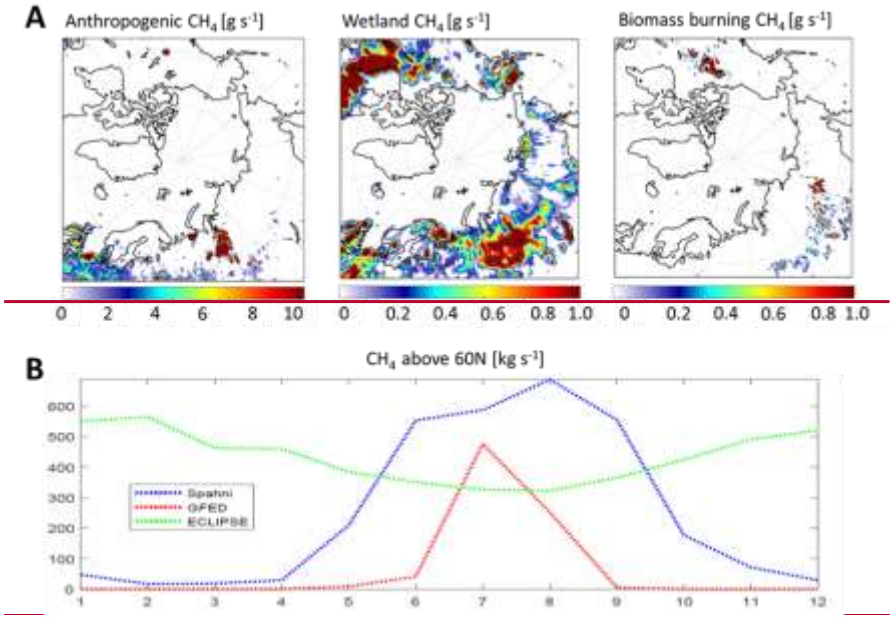
A
Anthropogenic CH4 [g s-1]
Wetland CH4 [g s-1]
Biomass burning CH4 [g s-1]
0 2 4 6 8 10
0 0.2 0.4 0.6 0.8 1.0
0 0.2 0.4 0.6 0.8 1.0
B
CH4 above 60N [kg s-1]
Spahni
GFED
ECLIPSE
600
500
400
300
200
100
0
1 2 3 4 5 6 7 8 9 10 11 12

1

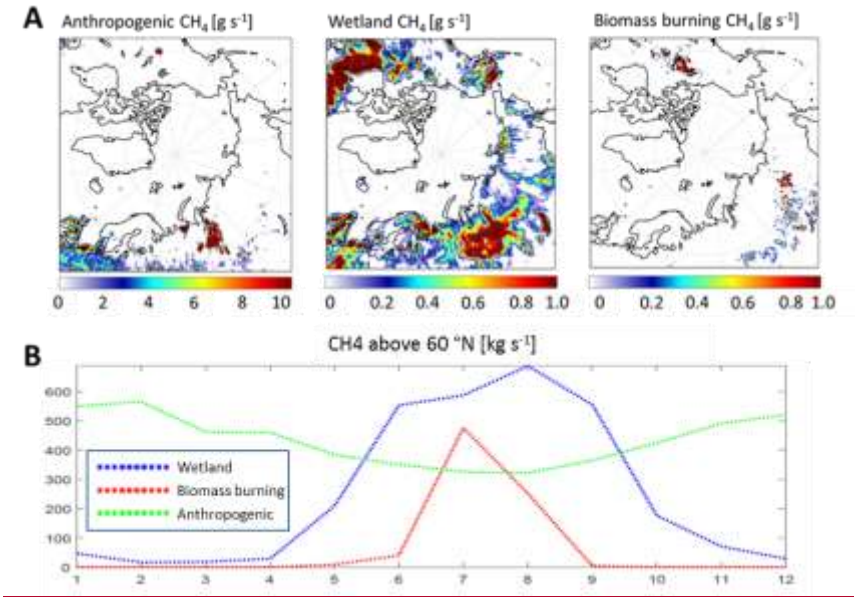

Figure 4: A) Annual average high latitude CH_4 emissions from anthropogenic sources, wetlands and biomass burning according to GAINS ECLIPSE (Stohl et al., 2015;http://www.iiasa.ac.at/web/home/research/researchPrograms/air/ECLIPSEv5a.html), LPX-Bern (Spahni et al., 2011;Stocker et al., 2014;www.climate.unibe.ch) and the Global Fire Emissions Database, GFED, (Randerson et al., 2017), respectively. B) Monthly variation in anthropogenic, wetland, and biomass burning emissions above 60°N

Formatted: Subscript

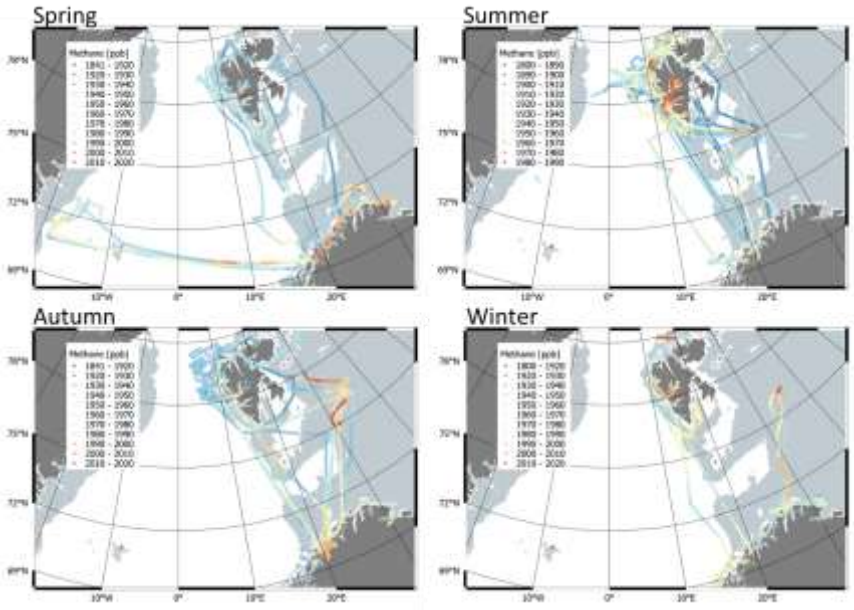

Figure 5: Methane mixing ratios observed at the RV Helmer Hanssen (colour scale), by location and plotted by calendar season (i.e. winter is December/ January/ February). Please note the change in colour scale between panels.

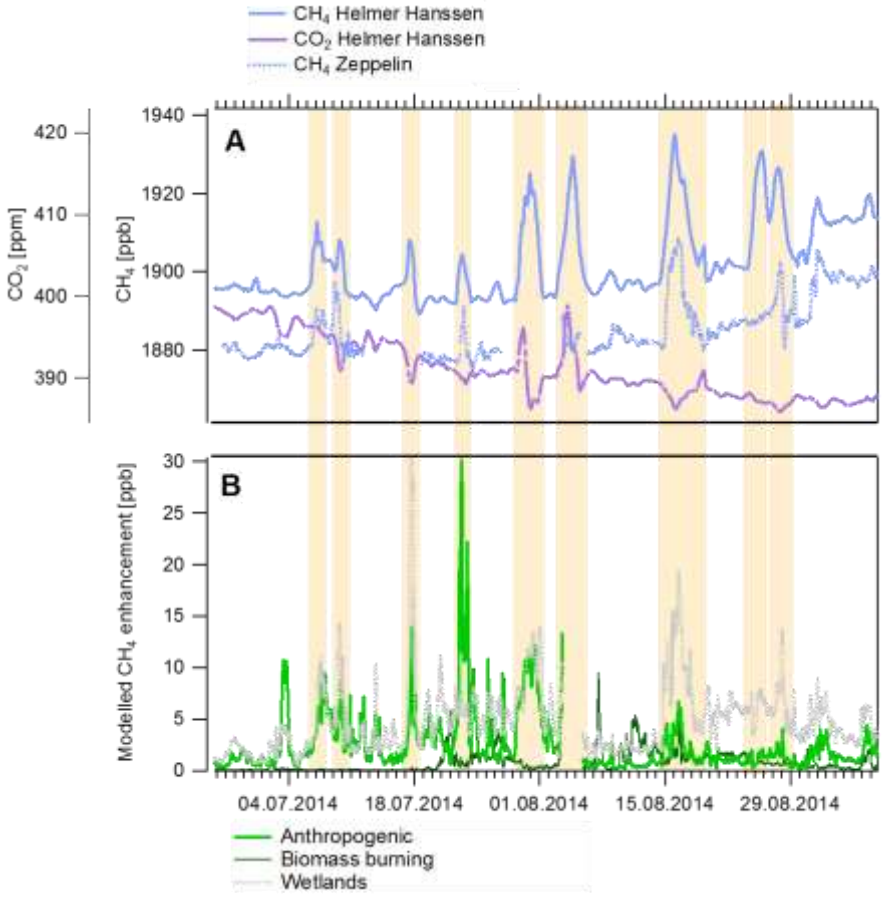

Figure 6: Example time series and model data presented in this study, from summer 2014 data. A) shows observation data of high time resolution (1 hour) methane (CH_4, light blue), carbon dioxide (CO_2, purple dashed) at the RV Helmer Hanssen and CH_4 at the Zeppelin for ship positions within 75-82° N, 5-35° E (blue dotted). B) Shows the modelled CH_4 enhancement due to anthropogenic activity (green), wetlands (grey) and biomass burning (dark green) according to emission inventories and FLEXPART (see text for details). Major excursions in the RV Helmer Hanssen CH_4 mixing ratio are highlighted.

Formatted: Subscript
Formatted: Subscript
Formatted: Subscript
Formatted: Subscript
Formatted: Subscript

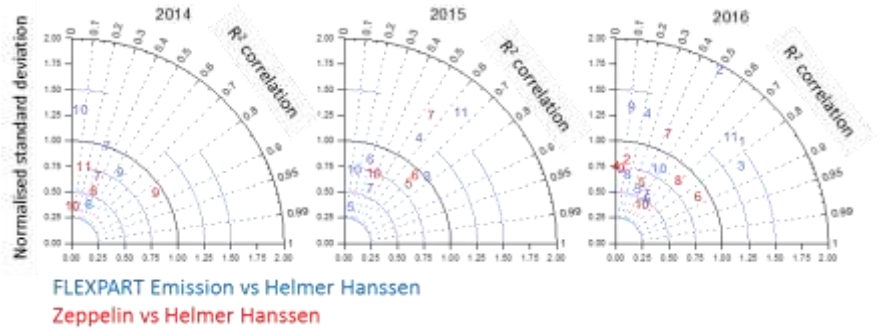

Figure 7: Taylor diagrams showing the monthly R^2 correlation (angle) and normalised standard deviation (radial axis) of modelled CH_4 emissions (blue) and CH_4 observed at Zeppelin Observatory (red, only for ship positions within 75-82° N, 5-35°) compared to the RV Helmer Hanssen CH_4 time series. Numbers refer to month of the year. Ideal agreement would be found at 1 on the radial axis (black line) and 1 on the angular axis.

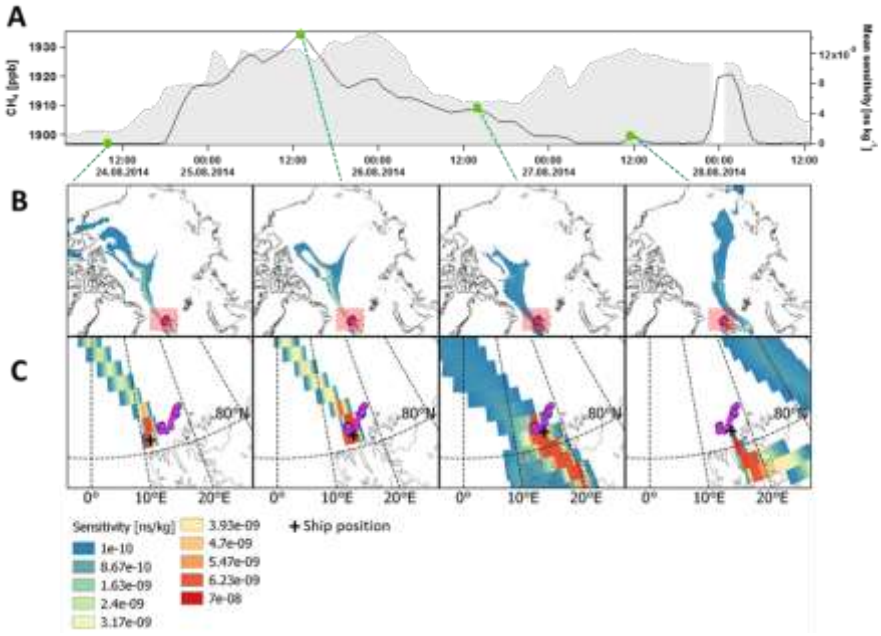

Figure 8: A) Methane (CH_4) measured North of Svalbard at the RV Helmer Hanssen shortly before, during, and after an episode of increased mixing ratios (grey shaded area) and mean footprint sensitivity (black line) to active flares located at 80.39-81.11°N,13.83-19°E, according to (Geissler et al., 2016), B) Regional FLEXPART footprint sensitivities in ns kg^{-1}, colour scale , and C) Local footprint FLEXPART sensitivities, for the area given by the red overview in B), including the locations of seabed gas flares, from (Geissler et al., 2016).

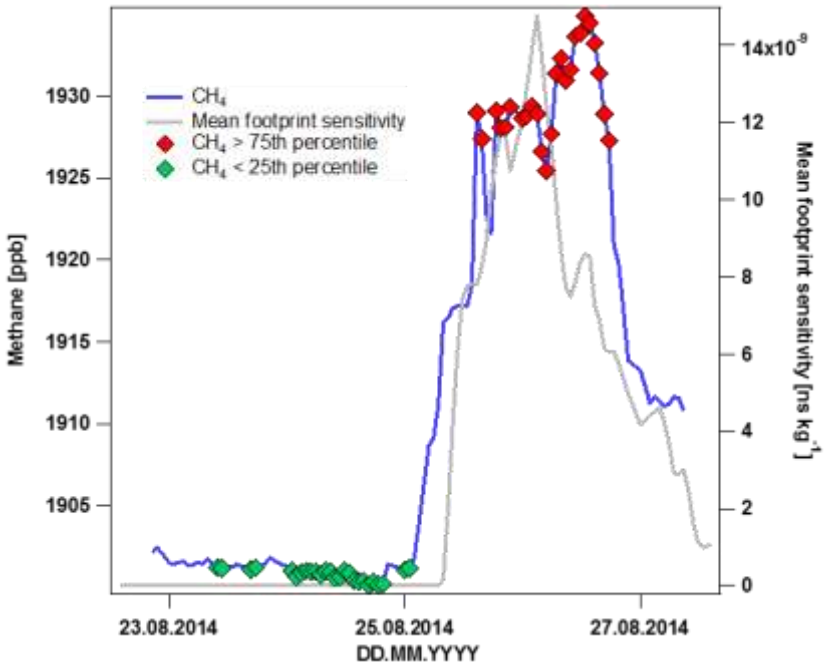

Figure 9: The methane (CH_4) atmospheric mixing ratio observed at the Helmer Hanssen north of Svalbard and mean footprint sensitivity to the active sub-sea seep region described by (Geissler et al., 2016), from 80.39-81.11°N, 13.83- 19°E (see also Fig. 8C), total area 3582.43 km^2. Points used to estimate a flux, i.e. ~~corresponding to~~ the highest CH_4 mixing ratios (above the 75th percentile) are shown in red and points corresponding to the lowest CH_4 mixing ratios (below the 25th percentile) are shown in green. Mean sensitivity to this area was determined using bilinear interpolation of the original 0.5°×0.5° FLEXPART footprint sensitivity field.

Formatted: Subscript